Genes and Environment, Vol. 33, No. 2 pp. 43-49 (2011)

Review

Perinatal Exposure to Environmental Chemicals Induces Epigenomic Changes in Offspring

Seiichiroh Ohsako[1]

Division of Environmental Health Sciences, Center for Disease Biology and Integrative Medicine, Graduate School and Faculty of Medicine, The University of Tokyo, Tokyo, Japan

(Received February 21, 2011; Revised March 10, 2011; Accepted March 10, 2011)

Many researchers propose that invisible internal alterations that occur through exposure to environmental factors during fetal or neonatal stages affect the risk of cancer, hypertension, and diabetes after maturation. Barker's hypothesis, which states that reduced fetal growth is strongly associated with metabolic syndromes including cardiovascular disease and diabetes, has now been widely accepted and expanded into the Developmental Origins of Health and Disease (DOHaD). Potential molecular mechanisms underlying this phenomenon include the alteration and persistence of epigenomic programming. Clear biochemical evidence has not yet been obtained in human studies; however, in laboratory animals, the fetal environment including physical and chemical factors altered epigenomic states such as DNA methylation and histone modification, and persistent changes affected specific gene expression regulation, resulting in disease susceptibility. Furthermore, in recent studies, environmental chemical exposure during pregnancy altered sperm DNA methylation patterns of male offspring, and the altered status and resulting phenotypes were inherited in the next generation. Challenging and eccentric studies focusing on epigenetic transgenerational effects are currently being conducted to demonstrate the existence of Lamarckian inheritance.

Key words: epigenetics, environmental chemical, DOHaD, acquired characteristics

Introduction

Recently, several researchers have proposed that invisible alterations that occur as a result of exposure to environmental factors during fetal or immature stages influence the risk of cancer, hypertension, and diabetes in adulthood. The molecular bases for disease susceptibilities are linked to epigenetics (1–5). Various environmental factors surrounding pregnant mothers and infants could be potential stimuli for epigenome alternation. For example, nutrient changes, exposure to environmental chemicals, and physical stresses such as insufficient care can alter the epigenome; thus, concern regarding chemicals that affect the health of the next generation has recently increased (6–9). In this review, several studies conducted on animals are presented to summarize the evidence that the fetal and neonatal environment can influence epigenomic modifications retained in later stages of life.

Epigenome Features and Mechanism of Their Structural Inheritance

In the field of epigenetic research, a considerable amount of attention has been paid to DNA methylation and histone modification because these processes are the most important epigenomic features. Variations in the amino acid acetylation/methylation status of histone octamers in the nucleosome of specific regions of chromatin and changes in DNA cytosine methylation patterns can be inherited by daughter cells after replication and cell division. Therefore, chromatin modification patterns are considered genetic information (epigenetic information or memory) (10).

DNA methylation typically occurs at CpG sites, which are 5′-CG-3′ dinucleotide sequences. Cytosine nucleotides of CpG are not methylated in newly synthesized DNA strands; thus, this double stranded state is called hemi-methylated DNA. Immediately after DNA replication, hemi-methylated DNA is recognized by Np95 (UHRF1) (11), which is a component of the replication factory complex. This complex contains proliferating cell nuclear antigen (PCNA) and DNA methyltransferase 1 (DNMT1), which transfers a methyl group to the 5 position of unmethylated cytosine in the newly synthesized opposite DNA strand (12,13). By this simple mechanism, information with methyl-CpG patterns (methylation status) is maintained in the nucleus of the daughter cell. CpG sites occur at a relatively low frequency in the genome. Because methyl-CpG sites are more susceptible to mutation and are lost over time,

[1]Correspondence to: Seiichiroh Ohsako, Division of Environmental Health Sciences, Center for Disease Biology and Integrative Medicine, Graduate School of Medicine, The University of Tokyo, 7-3-1 Hongo, Bunkyo-ku, Tokyo 113-8654, Japan. Tel: +81-3-5841-1432, Fax: +81-3-5841-1434, E-mail: ohsako@m.u-tokyo.ac.jp

CpG clusters or CpG islands are located on a specific region of the genome, i.e., gene promoter and exon 1. CpG methylation negatively regulates gene expression because transcription factors cannot bind methyl-CpG containing elements (14). Thereby, CpG islands of cell type specific regulatory genes are methylated followed by further chromatin modification. This chromatin remodeling including CpG methylation is highly correlated with cellular transformation and differentiation (15,16).

A histone octamer composed of one H2A, one H2B, two H3, and two H4 proteins is one unit of the nucleosome. Acetylation and methylation of acidic amino acid residues (lysine and arginine) in the amino-terminals of histone H3 and H4 are major epigenetic marks. In addition, phosphorylation, ubiquitination, sumoylation, ADP-ribosylation, and biotinylation are other chemical modifications of the histone tail (17). Histone acetylation and methylation are attuned to transcription activation and chromatin inactivation, respectively. Patterns of the covalent modifications of histone tails are extremely varied due to the number of modifiable amino acids and the possible combinations of substitution. Code information other than nucleotide sequences was advocated as the histone-code hypothesis; however, this theory is currently disregarded (18). Nevertheless, these histone-based modification patterns must influence region specific chromatin structure, resulting in differences in the level of gene expression. Many mechanistic models have been constructed to explain how histone modification patterns are inherited by daughter cells. In particular, a random distribution model is shown in Fig. 1 (19). On the newly synthesized DNA, parental histone H3–H4 tetramers are reused for the formation of the nucleosome of daughter chromatin. At the same time, newly synthesized histone H3–H4 tetramers are incorporated into the daughter nucleosome at random. Newly synthesized histone marks, e.g., acetylated lysine, are erased by histone deacetylases (HDACs). Methylated marks derived from parental histones that are next to newly incorporated histones are recognized by heterochromatin protein 1 (HP1), which forms a complex with histone methyltransferase (HMT). Subsequently, erased marks in the newly incorporated histones are quickly methylated by HMT. In this manner, histone modification patterns in a specific region of the genome are precisely copied. In addition, a semi-conservative model in which only dimers of H3–H4 tetramer are reused during nucleosome formation and an asymmetric model in which interactions between two newly synthesized DNA strands have been proposed for the regulation of histone modification copying (10,18,19).

Other than DNA methylation and histone modification, non-coding RNA, microRNA, and polycomb group (PcG) protein complex are epigenetic factors that modulate chromatin higher structure and influence the cellular phenotype (20,21). These varieties of macromolecular architectures may regulate and integrate epigenome inheritance.

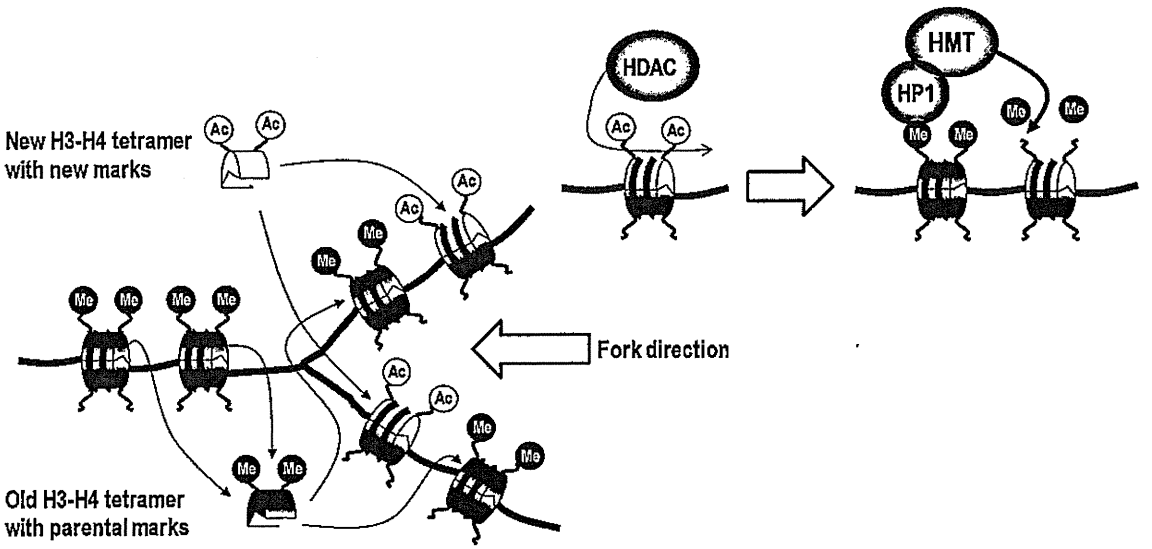

Fig. 1. A mechanistic representation of a hypothetical example of histone modification pattern inheritance. On newly synthesized DNA, parental histone H3–H4 tetramers are reused for the formation of the nucleosome of daughter chromatin. At the same time, newly synthesized histone H3–H4 tetramers are incorporated at random. The new histone marks (e.g., acetylated lysine) are erased by HDACs. Methylated marks derived from parental histones neighboring newly incorporated histones are recognized by HP1, which forms a complex with HMT. Erased marks in the newly incorporated histones are quickly methylated by HMT. In this manner, histone modification patterns in a specific region of the genome are precisely copied (19).

Human Disease and Epigenetics

In the retrospective cohort studies of David Barker and colleagues conducted in the United Kingdom, in which the country was divided into 212 local authority areas, a strong geographical relationship was observed between ischaemic heart disease mortality rates in 1968–78 and infant mortality in 1921–25 (1). Based on detailed epidemiological studies regarding the relationship between mother's birth weight and blood pressure, they concluded that babies who were small at birth or during infancy displayed increased rates of cardiovascular disease in adulthood (2). Moreover, they proposed the thrifty phenotype hypothesis, in which epidemiological associations between poor fetal and infant growth and the subsequent development of type 2 diabetes and metabolic syndrome are due to the effects of poor nutrition in early life, which produces permanent changes in glucose-insulin metabolism (22). The aforementioned theory is Barker's hypothesis, in which low maternal nutrition causes metabolic syndrome in offspring. Later termed the Developmental Origins of Health and Disease (DOHaD), the theory was expanded from Barker's hypothesis into the more general theory that health and disease susceptibility in the next generation depends on the environment surrounding the fertilized egg and fetuses in uterus, and throughout the neonatal life time (3,4,23).

Several attempts have recently been made to explain this phenomenon. The most reliable molecular mechanism underlying DOHaD is that epigenetic alternations that occur during the sensitive stage of fetus and newborn development persist into adulthood (5). In human studies, clear biochemical evidence has not yet been obtained; however, in laboratory animal experiments, the fetal environment, including physical and chemical factors altered epigenomic states such as DNA methylation and histone modification and persistent changes, influenced specific gene expression regulation (5). DOHaD has become more than a hypothesis and has been accepted by the clinical field. In the next section, animal studies related to DOHaD will be described.

Many carcinogeneses are known to be caused by aberrant DNA methylation, which is partially acquired in later stages of development. The hypermethylation of tumor suppressor genes such as *pRB* or *p16* is involved in retinoblastoma and epigenetic carcinogenesis (24,25). Clinical researchers are now considering epigenetic aberrations during carcinogenesis because DNA methyltransferase inhibitors are useful for cancer therapy (26–28). Thus, concern about chemically-induced epigenetic carcinogenesis in the next generation is increasing (6,8).

Animal Models Representing Epigenomic Changes Due to Perinatal Environmental Factors

Recently, a number of reports based on experimental animal models such as rats and mice demonstrated that *in utero* or neonatal nursing environmental stimuli altered DNA methylation and histone modification, which can persist into adulthood and potentially influence the phenotype (5,29). In most of these reports, clear and significant changes in the epigenome of specific target genes were detected. As described briefly below, in many of these reports, environmental chemicals including endocrine disruptors, which do not have mutagenic activities, were evaluated. Several leading papers are summarized in Table 1.

In rats, naturally occurring variations in maternal care influence the sensitivity of offspring to stress in adulthood. Meaney and colleagues at McGill University reported that the offspring of mothers that exhibited more licking and grooming of pups showed reduced plasma adrenocorticotropic hormone and corticosterone responses to acute stress, increased hippocampal glucocorticoid receptor (GR) mRNA expression, and enhanced glucocorticoid feedback sensitivity (30). Increased pup licking and grooming and arched-back nursing by rat mothers altered the offspring epigenome at a *Gr* gene promoter in the hippocampus, i.e., hypomethyaltion of CpG and increased histone acetylation and transcription factor (NGFI-A) binding (31). These studies revealed that maternal care determines offspring stress resistance in adulthood due to an altered level of epigenomic states in the brain.

Viable yellow (A^{vy}) mice are larger, obese, hyperinsulinemic, more susceptible to cancer, and shorter lived than their non-yellow siblings (32). They are epigenetic mosaics ranging from a yellow phenotype with maximum ectopic *Agouti* gene overexpression through a continuum of mottled *Agouti/yellow* phenotypes with partial *Agouti* overexpression to a pseudoagouti phenotype with minimal ectopic expression (32,33). This marked phenotypic change is significantly associated with the methylation level of CpG sites in an intracisternal A particle (IAP) retrotransposon upstream of the transcription start site of the *Agouti* gene. Feeding pregnant dams methyl-supplemented diets alters the epigenetic regulation of *Agouti* expression in their offspring, as indicated by increased *Agouti/black* mottling in the direction of the pseudoagouti phenotype (34). Maternal dietary genistein supplementation shifted the coat color of heterozygous viable yellow offspring toward pseudoagouti by hypermethylation of CpG sites in the retrotransposon of the *Agouti* gene (35). Furthermore, maternal exposure to bisphenol-A, an endocrine disruptor, shifted the coat color toward yellow by hypomethylation of retrotransposon CpG sites. Moreover, mater-

Table 1. Leading reports describing transgenerational effects of chemical exposures on epigenomic alternations in experimental animal models

Report	Animal	Chemicals	Dose	Period of exposure	Observed effects on phenotype	Detected changes in DNA methylation
Wu *et al.* (39)	ICR mouse	2,3,7,8-tetrachloro dibenzo-*p*-dioxin	10 nM *in vitro*	Fertilized egg with 1–2 cell or in the 8-cell stage	Reduced fetal body weight and reduced H19 mRNA expression	Hypermethyation of *H19/Igf2* genomic imprint region of DNA from the fetal body
Anway *et al.* (50) Crews *et al.* (52)	Sprague-Dawly rats	Vinclozolin Methoxychlor	100 mg/kg/day mother bw ip (Vinclozolin) 200 mg/kg/day mother bw ip (Methoxychlor)	Day 8 to day 15 of gestation	Germ cell apoptosis, decreased sperm count, decreased sexual preference for normal females in male offspring (F1–F4)	Hypomethylation of *Lplase* and cytokine-inducible SH2 protein genes in sperm DNA
Dolinoy *et al.* (35)	A^{vy} mouse	Genistein	250 mg/kg diet	2 weeks before mating through weaning	Coat-color change (a decease in yellow color and an increase pseudoagouti phenotype)	Hypermethylation of IAP insertion of the *Agouti* gene promoter region in skin DNA
Dolinoy *et al.* (36)	A^{vy} mouse	Bisphenol-A	50 mg/kg diet	2 weeks before mating through weaning	Coat-color change (an increase in yellow color and a decrease in the pseudoagouti phenotype)	Hypomethylation of IAP insertion of the *Agouti* gene promoter region in skin DNA
Onishchenko *et al.* (38)	C57BL/6kl mouse	Methylmercury	0.5 mg/kg/day via drinking water	Day 7 of gestation to day 7 of the postnatal period	Depression-like behavior and hippocampal BDNF mRNA suppression	Hypermethyaltion of hippocampal *Bdnf* promoter
Bromer *et al.* (37)	CD-1 mouse	Diethylstilbestrol	10 μg/kg/day mother bw ip	Day 9 to day 16 of gestation	Abnormalities in the reproductive tract and decreased homeobox A10 expression	Hypermethyaltion of uterus homeobox A10 gene intron

nal dietary supplementation with methyl donors such as folic acid or genistein negated the DNA hypomethylating effect of bisphenol-A (36).

Diethylstilbestrol (DES), a nonsteroidal estrogen, induces developmental anomalies in the female reproductive tract including vaginal cancer in humans perinatally exposed to DES. The expression of homeobox gene *Hoxa10*, which controls uterine organogenesis, is repressed in DES-exposed mouse offspring (37). In the mouse model, CpG methylation frequency in the *Hoxa10* intron was greater in DES-exposed offspring than control mice and was accompanied by increased expression of DNMT1 and DNMT3b.

Perinatal exposure to methylmercury causes persistent changes in learning and motivational behavior in C57BL/6 mice. Behavioral alterations are associated with a decrease in brain-derived neurotrophic factor (BDNF) mRNA in the hippocampal dentate gyrus. In this mouse experiment, methylmercury exposure caused the chromatin structure at the *Bdnf* promoter region to enter into a long-lasting repressive state. In particular, DNA hypermethylation, an increase in histone H3-K27 tri-methylation, and a decrease in H3 acetylation were observed at promoter IV (38).

2,3,7,8-Tetrachlorodibenzo-*p*-dioxin (TCDD) is the most toxic environmental pollutant. Short term exposure of preimplantation ICR mouse embryos to TCDD (10 nM) during the 1-cell stage to the blastocyst stage resulted in reduced fetal weight compared to unexposed preimplanted embryos. A decrease in the level of expression of imprinted genes *H19* and *Igf2* was observed, along with in an increase in the methylation frequency of the *H19/Igf2* imprint control region due to an increase in the paternal methylation status (39).

Perinatal exposure to a low dose of TCDD (environmental contamination levels) induces various types of developmental abnormalities in the offspring of laboratory animals (40,41). The cellular target molecule is an arylhydrocarbon receptor (AHR), which mediates every outcome of low dose TCDD toxicity (42). AHR can bind to polycyclic aromatic hydrocarbon mutagens such as benzo[*a*]pyrene (BaP) and 7,12-dimethylbenz[*a*]anthracene (DMBA) and can transactivate downstream target genes, including cytochrome P450 (CYP) family 1A1 and 1B1, which are phase I drug metabolizing enzymes (43). Using its monooxygenase activity, CYPs convert the mutagen into a reactive epoxide, which produces a covalent bond to the guanine residue in DNA and results in nucleotide mutation (44). In contrast, TCDD is a stable compound in the environment and living bodies; thus, TCDD cannot bind to DNA directly and induce mutations in nucleotide sequences. Female Sprague-Dawley rats exposed to TCDD in the fetal stage were more prone to DMBA-induced mammary tumors in adulthood than control rats

(45). Very low doses of 3,3′,4,4′,5-pentachlorobiphenyl (PCB126), which has a similar bioactivity to that of TCDD, had the same effect on DMBA-induced mammary tumor models when administered during pregnancy (46). Moreover, the induction state of *Cyp1a1* and *Cyp1b1* genes in the liver were enhanced after DMBA injection (47). The acceleration of *Cyp1* transcription resulted in higher carcinogenic susceptibility due to epigenetic alternations. In our laboratory, we demonstrated that C57BL/6J mice administered TCDD during the fetal stage showed a higher incidence of forestomach cancer due to BaP injection and enhanced induction of Cyp1a1 mRNA by TCDD re-administration in adulthood. Methyl-CpGs level of the *Cyp1a1* promoter region, which includes Ahr-binding xenobiotic response elements, is involved in TCDD induced transcription activity in LNCaP cells (48). The methylation frequency of the *Cyp1a1* promoter region in the liver DNA of mice exposed to TCDD was significantly lower than that of the control mice. Moreover, acetylation levels of histone H3 and H4 were significantly higher in TCDD-exposed mice (unpublished observations).

In laboratory studies conducted on animals, substantial evidence suggests that perinatal exposure to chemicals alters the epigenetic program of sensitive organs and persists into adulthood, affecting disease susceptibility. The mechanism of epigenomic status modulation, CpG hyper/hypomethylation, and maintenance of increased histone acetylation/methylation is still unclear; however, investigations are currently being conducted by many researchers.

Transgenerational Effects and Possible Lamarckian Inheritance

According to Barker's hypothesis, offspring phenotypes such as cardiovascular disease, risk of cancer, hypertension, and diabetes are thought to be inherited by the next generation (49). The epigenome alternations summarized in the present review can be inherited by the later generation via germ cell lines. Skinner and colleagues at Washington State University administered endocrine disruptors, fungicide vinclozolin and pesticide methoxychlor, to pregnant Sprague-Dawley rats to investigate spermatogenic defects and other toxic endpoints in male offspring (50). Transient exposure of vinclozolin, which does not display mutagenic activity, induced decreased spermatogenic capacity in adult phenotypes of the F_1 generation (sperm count and viability) and increased incidence of male infertility. These effects were transferred through the male germ line to nearly all of the males of subsequent generations, i.e., F_1 to F_4 (50,51). Moreover, male rats whose progenitors had been treated with vinclozolin showed lowered mate preference from control females (52). Using an arbitrary primer PCR and methylation sensitive restriction enzyme *Hpa*II, the authors demonstrated that the methylation pattern of lysophospholipase (*Lplase*) and cytokine-inducible SH2 protein genes was altered in the epididymal sperm DNA of F_2 and F_3 animals (50). Most recently, using a methylated DNA immunoprecipitation technique based on methyl-cytosine antibodies and a promoter tilling microarray (MeDIP-Chip) procedure, Skinner and coworkers identified 52 different regions in the sperm promoter epigenome with altered methylation patterns due to maternal exposure of vinclozolin (53). The series of studies conducted by Skinner's group suggest that a phenotype can be acquired by maternal exposure to environmental factors, leading to evolutional changes in animals. However, these studies are somewhat controversial because experiments focused on *Lplase* gene hypomethylation have not been reproduced using an identical protocol (54).

Compared to the offspring of males fed a control diet, the offspring of males fed a low-protein diet exhibited elevated hepatic expression of many genes involved in lipid and cholesterol biosynthesis and decreased levels of cholesterol esters (55). Epigenomic profiling of offspring livers via deep sequencing technology revealed numerous changes in CpG methylation due to alterations in the paternal diet, including reproducible changes in methylation over a likely enhancer for *Ppara*, a key lipid regulator. The results indicated that the parental diet can affect cholesterol and lipid metabolism in offspring, and a model system to study the environmental reprogramming of the heritable epigenome was defined. Acquired characteristics in the next generation may be inherited through the epigenome of paternal germlines. However, differences in sperm DNA methylation were not detected via deep sequencing (55). The epigenetic inheritance of RNA molecules has been described, and the expression of unusual *Kit* RNAs in the male germline (spermatozoon) of mice resulted in a phenotypic effect (on coat color) on the progeny of affected mice. In particular, two genetically identical mice differed phenotypically based on their parents' genotypes (56). These reports imply that untranslated RNAs can be potent epigenetic modulators for transgenerational effects on acquired characteristics rather than DNA methylation (57).

In the middle of the last century, Lysenko, a Russian plant biologist, emphasized his theory by conducting nutritional hybrid experiments and suggested that a white albino tomato could be transformed into a red tomato. Moreover, he suggested that autumn wheat could become spring wheat by applying low temperature treatments; however, little evidence was presented in these experiments. The aforementioned work was based on Lemarckian inheritance, i.e., the inheritance of an acquired phenotype. The theories of Lamarck and Lysenko have been neglected in the twentieth century.

However, the name of Lysenko, a very infamous one, is rising again in this century, due to the growth of epigenetics (58). Epigenetic transgenerational effects may alter germlines, and unknown factors other than DNA methylation or non-coding RNAs may be involved. The progress of research on acquired phenotypes will have a significant effect on perinatal medical aspects.

Acknowledgments: The author gratefully acknowledge Dr Kayoko Shimoi of the University of Shizuoka and Dr Tohru Shibuya for providing the opportunity to submit the manuscript to Genes and Environment.

References

1 Barker DJ, Osmond C. Infant mortality, childhood nutrition, and ischaemic heart disease in England and Wales. Lancet. 1986; 1: 1077–81.
2 Barker DJ, Shiell AW, Barker ME, Law CM. Growth *in utero* and blood pressure levels in the next generation. J Hypertens. 2000; 18: 843–6.
3 Sinclair KD, Lea RG, Rees WD, Young LE. The developmental origins of health and disease: current theories and epigenetic mechanisms. Soc Reprod Fertil Suppl. 2007; 64: 425–43.
4 Swanson JM, Entringer S, Buss C, Wadhwa PD. Developmental origins of health and disease: environmental exposures. Semin Reprod Med. 2009; 27: 391–402.
5 Rosenfeld CS. Animal models to study environmental epigenetics. Biol Reprod. 2010; 82: 473–88.
6 LeBaron MJ, Rasoulpour RJ, Klapacz J, Ellis-Hutchings RG, Hollnagel HM, Gollapudi BB. Epigenetics and chemical safety assessment. Mutat Res. 2010; 705: 83–95.
7 Bernal AJ, Jirtle RL. Epigenomic disruption: the effects of early developmental exposures. Birth Defects Res A Clin Mol Teratol. 2010; 88: 938–44.
8 Goodman JI, Augustine KA, Cunnningham ML, Dixon D, Dragan YP, Falls JG, Rasoulpour RJ, Sills RC, Storer RD, Wolf DC, Pettit SD. What do we need to know prior to thinking about incorporating an epigenetic evaluation into safety assessments? Toxicol Sci. 2010; 116: 375–81.
9 Ho DH, Burggren WW. Epigenetics and transgenerational transfer: a physiological perspective. J Exp Biol. 2010; 213: 3–16.
10 Corpet A, Almouzni G. Making copies of chromatin: the challenge of nucleosomal organization and epigenetic information. Trends Cell Biol. 2009; 19: 29–41.
11 Bostick M, Kim JK, Esteve PO, Clark A, Pradhan S, Jacobsen SE. UHRF1 plays a role in maintaining DNA methylation in mammalian cells. Science. 2007; 317: 1760–4.
12 Bestor T, Laudano A, Mattaliano R, Ingram V. Cloning and sequencing of a cDNA encoding DNA methyltransferase of mouse cells. The carboxyl-terminal domain of the mammalian enzymes is related to bacterial restriction methyltransferases. J Mol Biol. 1988; 203: 971–83.
13 Iida T, Suetake I, Tajima S, Morioka H, Ohta S, Obuse C, Tsurimoto T. PCNA clamp facilitates action of DNA cytosine methyltransferase 1 on hemimethylated DNA. Genes Cells. 2002; 7: 997–1007.
14 Comb M, Goodman HM. CpG methylation inhibits proenkephalin gene expression and binding of the transcription factor AP-2. Nucleic Acids Res. 1990; 18: 3975–82.
15 Rideout WM 3rd, Eversole-Cire P, Spruck CH 3rd, Hustad CM, Coetzee GA, Gonzales FA, Jones PA. Progressive increases in the methylation status and heterochromatinization of the myoD CpG island during oncogenic transformation. Mol Cell Biol. 1994; 14: 6143–52.
16 Reik W, Dean W, Walter J. Epigenetic reprogramming in mammalian development. Science. 2001; 293: 1089–93.
17 Shilatifard A. Chromatin modifications by methylation and ubiquitination: implications in the regulation of gene expression. Annu Rev Biochem. 2006; 75: 243–69.
18 Turner BM. Cellular memory and the histone code. Cell. 2002; 111: 285–91.
19 Probst AV, Dunleavy E, Almouzni G. Epigenetic inheritance during the cell cycle. Nat Rev Mol Cell Biol. 2009; 10: 192–206.
20 Djupedal I, Ekwall K. Epigenetics: heterochromatin meets RNAi. Cell Res. 2009; 19: 282–95.
21 Francis NJ. Mechanisms of epigenetic inheritance: copying of polycomb repressed chromatin. Cell Cycle. 2009; 8: 3513–8.
22 Hales CN, Barker DJ. The thrifty phenotype hypothesis. Br Med Bull. 2001; 60: 5–20.
23 Wadhwa PD, Buss C, Entringer S, Swanson JM. Developmental origins of health and disease: brief history of the approach and current focus on epigenetic mechanisms. Semin Reprod Med. 2009; 27: 358–68.
24 Ohtani-Fujita N, Dryja TP, Rapaport JM, Fujita T, Matsumura S, Ozasa K, Watanabe Y, Hayashi K, Maeda K, Kinoshita S, Matsumura T, Ohnishi Y, Hotta Y, Takahashi R, Kato MV, Ishizaki K, Sasaki MS, Horsthemke B, Minoda K, Sakai T. Hypermethylation in the retinoblastoma gene is associated with unilateral, sporadic retinoblastoma. Cancer Genet Cytogenet. 1997; 98: 43–9.
25 Esteller M. CpG island hypermethylation and tumor suppressor genes: a booming present, a brighter future. Oncogene. 2002; 21: 5427–40.
26 McCabe MT, Low JA, Daignault S, Imperiale MJ, Wojno KJ, Day ML. Inhibition of DNA methyltransferase activity prevents tumorigenesis in a mouse model of prostate cancer. Cancer Res. 2006; 66: 385–92.
27 Ushijima T. Detection and interpretation of altered methylation patterns in cancer cells. Nat Rev Cancer. 2005; 5: 223–31.
28 Ushijima T, Asada K. Aberrant DNA methylation in contrast with mutations. Cancer Sci. 2010; 101: 300–5.
29 McMullen S, Mostyn A. Animal models for the study of the developmental origins of health and disease. Proc Nutr Soc. 2009; 68: 306–20.
30 Liu D, Diorio J, Tannenbaum B, Caldji C, Francis D, Freedman A, Sharma S, Pearson D, Plotsky PM, Meaney MJ. Maternal care, hippocampal glucocorticoid receptors, and hypothalamic-pituitary-adrenal responses to

stress. Science. 1997; 277: 1659–62.
31 Weaver IC, Cervoni N, Champagne FA, D'Alessio AC, Sharma S, Seckl JR, Dymov S, Szyf M, Meaney MJ. Epigenetic programming by maternal behavior. Nat Neurosci. 2004; 7: 847–54.
32 Yen TT, Gill AM, Frigeri LG, Barsh GS, Wolff GL. Obesity, diabetes, and neoplasia in yellow A(vy)/-mice: ectopic expression of the agouti gene. Faseb J. 1994; 8: 479–88.
33 Wolff GL, Kodell RL, Moore SR, Cooney CA. Maternal epigenetics and methyl supplements affect agouti gene expression in Avy/a mice. Faseb J. 1998; 12: 949–57.
34 Waterland RA, Jirtle RL. Transposable elements: targets for early nutritional effects on epigenetic gene regulation. Mol Cell Biol. 2003; 23: 5293–300.
35 Dolinoy DC, Weidman JR, Waterland RA, Jirtle RL. Maternal genistein alters coat color and protects Avy mouse offspring from obesity by modifying the fetal epigenome. Environ Health Perspect. 2006; 114: 567–72.
36 Dolinoy DC, Huang D, Jirtle RL. Maternal nutrient supplementation counteracts bisphenol A-induced DNA hypomethylation in early development. Proc Natl Acad Sci USA. 2007; 104: 13056–61.
37 Bromer JG, Wu J, Zhou Y, Taylor HS. Hypermethylation of homeobox A10 by *in utero* diethylstilbestrol exposure: an epigenetic mechanism for altered developmental programming. Endocrinology. 2009; 150: 3376–82.
38 Onishchenko N, Karpova N, Sabri F, Castren E, Ceccatelli S. Long-lasting depression-like behavior and epigenetic changes of BDNF gene expression induced by perinatal exposure to methylmercury. J Neurochem. 2008; 106: 1378–87.
39 Wu Q, Ohsako S, Ishimura R, Suzuki JS, Tohyama C. Exposure of mouse preimplantation embryos to 2,3,7,8-tetrachlorodibenzo-*p*-dioxin (TCDD) alters the methylation status of imprinted genes *H19* and *Igf2*. Biol Reprod. 2004; 70: 1790–7.
40 Mably TA, Moore RW, Goy RW, Peterson RE. *In utero* and lactational exposure of male rats to 2,3,7,8-tetrachlorodibenzo-p-dioxin. 2. Effects on sexual behavior and the regulation of luteinizing hormone secretion in adulthood. Toxicol Appl Pharmacol. 1992; 114: 108–17.
41 Ohsako S, Miyabara Y, Sakaue M, Ishimura R, Kakeyama M, Izumi H, Yonemoto J, Tohyama C. Developmental stage-specific effects of perinatal 2,3,7,8-tetrachlorodibenzo-*p*-dioxin exposure on reproductive organs of male rat offspring. Toxicol Sci. 2002; 66: 283–92.
42 Ohsako S, Fukuzawa N, Ishimura R, Kawakami T, Wu Q, Nagano R, Zaha H, Sone H, Yonemoto J, Tohyama C. Comparative contribution of the aryl hydrocarbon receptor gene to perinatal stage development and dioxin-induced toxicity between the urogenital complex and testis in the mouse. Biol Reprod. 2010; 82: 636–43.
43 Whitlock JP Jr. Induction of cytochrome P4501A1. Annu Rev Pharmacol Toxicol. 1999; 39: 103–25.
44 Sims P, Grover PL, Swaisland A, Pal K, Hewer A. Metabolic activation of benzo[*a*]pyrene proceeds by a diol-epoxide. Nature. 1974; 252: 326–8.
45 Brown NM, Manzolillo PA, Zhang JX, Wang J, Lamartiniere CA. Prenatal TCDD and predisposition to mammary cancer in the rat. Carcinogenesis. 1998; 19: 1623–9.
46 Muto T, Wakui S, Imano N, Nakaaki K, Takahashi H, Hano H, Furusato M, Masaoka T. Mammary gland differentiation in female rats after prenatal exposure to 3,3′,4,4′,5-pentachlorobiphenyl. Toxicology. 2002; 177: 197–205.
47 Wakui S, Yokoo K, Takahashi H, Muto T, Suzuki Y, Kanai Y, Hano H, Furusato M, Endou H. Prenatal 3,3′,4,4′,5-pentachlorobiphenyl exposure modulates induction of rat hepatic CYP 1A1, 1B1, and AhR by 7,12-dimethylbenz[*a*]anthracene. Toxicol Appl Pharmacol. 2006; 210: 200–11.
48 Okino ST, Pookot D, Li LC, Zhao H, Urakami S, Shiina H, Igawa M, Dahiya R. Epigenetic inactivation of the dioxin-responsive cytochrome P4501A1 gene in human prostate cancer. Cancer Res. 2006; 66: 7420–8.
49 Jirtle RL, Skinner MK. Environmental epigenomics and disease susceptibility. Nat Rev Genet. 2007; 8: 253–62.
50 Anway MD, Cupp AS, Uzumcu M, Skinner MK. Epigenetic transgenerational actions of endocrine disruptors and male fertility. Science. 2005; 308: 1466–9.
51 Skinner MK, Anway MD. Seminiferous cord formation and germ-cell programming: epigenetic transgenerational actions of endocrine disruptors. Ann N Y Acad Sci. 2005; 1061: 18–32.
52 Crews D, Gore AC, Hsu TS, Dangleben NL, Spinetta M, Schallert T, Anway MD, Skinner MK. Transgenerational epigenetic imprints on mate preference. Proc Natl Acad Sci USA. 2007; 104: 5942–6.
53 Guerrero-Bosagna C, Settles M, Lucker B, Skinner MK. Epigenetic transgenerational actions of vinclozolin on promoter regions of the sperm epigenome. PLoS One. 2010; 5: e13100.
54 Inawaka K, Kawabe M, Takahashi S, Doi Y, Tomigahara Y, Tarui H, Abe J, Kawamura S, Shirai T. Maternal exposure to anti-androgenic compounds, vinclozolin, flutamide and procymidone, has no effects on spermatogenesis and DNA methylation in male rats of subsequent generations. Toxicol Appl Pharmacol. 2009; 237: 178–87.
55 Carone BR, Fauquier L, Habib N, Shea JM, Hart CE, Li R, Bock C, Li C, Gu H, Zamore PD, Meissner A, Weng Z, Hofmann HA, Friedman N, Rando OJ. Paternally induced transgenerational environmental reprogramming of metabolic gene expression in mammals. Cell. 2010; 143: 1084–96.
56 Rassoulzadegan M, Grandjean V, Gounon P, Vincent S, Gillot I, Cuzin F. RNA-mediated non-mendelian inheritance of an epigenetic change in the mouse. Nature. 2006; 441: 469–74.
57 Rando OJ, Verstrepen KJ. Timescales of genetic and epigenetic inheritance. Cell. 2007; 128: 655–68.
58 Maderspacher F. Lysenko rising. Curr Biol. 2010; 20: R835–7.

ANATOMIA HISTOLOGIA EMBRYOLOGIA
JOURNAL OF VETERINARY MEDICINE

Anatomia Histologia Embryologia

ORIGINAL ARTICLE

Di(*n*-butyl) Phthalate Induces Vimentin Filaments Disruption in Rat Sertoli Cells: A Possible Relation with Spermatogenic Cell Apoptosis

M. S. Alam[1], S. Ohsako[2], T. W. Tay[1], N. Tsunekawa[1], Y. Kanai[1] and M. Kurohmaru[1]*

Addresses of authors: [1] Department of Veterinary Anatomy, Graduate School of Agricultural and Life Sciences, The University of Tokyo, 1-1-1 Yayoi, Bunkyo-ku, Tokyo 113-8657, Japan;
[2] Laboratory of Environmental Health Sciences, Center for Disease Biology and Integrative Medicine, Graduate School and Faculty of Medicine, The University of Tokyo, 7-3-1 Hongo, Bunkyo-ku, Tokyo 113-0033

***Correspondence:**
Tel.: +81 (3) 5841 5384;
fax: +81 (3) 5841 8181,
e-mail: amkuroh@mail.ecc.u-tokyo.ac.jp

With 3 figures

Received January 2010; accepted for publication January 2010

doi: 10.1111/j.1439-0264.2010.00993.x

Summary

Phthalate esters have been extensively used as a plasticizer of synthetic polymers. Previous studies have revealed that some phthalate esters including di(*n*-butyl) phthalate (DBP) induce spermatogenic cell apoptosis, although its mechanism is not yet clear. The present study describes that disruption of Sertoli cell vimentin filaments by DBP administration may relate to spermatogenic cell apoptosis. The present histopathological study revealed that a single oral administration of 500 mg/kg DBP caused progressive detachment and displacement of spermatogenic cells away from the seminiferous epithelium and sloughing of them into the lumen. Degenerative spermatogenic cells characterized by chromatin condensation were frequently observed in DBP-treated rats. Ultrastructurally, the degenerative spermatogenic cells were separated from their neighbours, and a collapse of Sertoli cell vimentin filaments was recognized in DBP-treated rats. Sertoli cell cultures showed the increased number and size of vacuoles in their cytoplasm. In agreement with the *in vivo* experiment, vimentin filaments clearly showed a gradual collapse in DBP-exposed Sertoli cells *in vitro*. These *in vivo* and *in vitro* experiments indicate that DBP-induced collapse of Sertoli cell vimentin filaments may lead to detachment of spermatogenic cells, and then detached cells may undergo apoptosis because of loss of the support and nurture provided by Sertoli cells.

Introduction

Di(*n*-butyl) phthalate (DBP), one of heavily used phthalate esters, is widely used as a plasticizer in cosmetics, printing inks and pharmaceutical coating. Phthalate esters including DBP have been shown to induce testicular atrophy. To date, several mechanisms have been proposed to explain the induction of testicular atrophy by phthalate esters. For example, the depletion of zinc in testes was induced by monobutyl phthalate (MBP) and mono(2-ethylhexyl) phthalate (MEHP), metabolites of DBP and di(2-ethylhexyl) phthalate (DEHP), respectively (Oishi and Hiraga, 1980). Membrane alteration of Sertoli cells induced by MEHP would lead to separation of spermatogenic cells from underlying Sertoli cells (Gray and Beamand, 1984; Richburg and Boekelheide, 1996; Tay et al., 2007). Upregulation of Fas and Fas ligand gene induced by MEHP activated spermatogenic cell apoptosis (Lee et al., 1997; 1999; Richburg et al., 1999). However, the primary cellular target or mechanism of DBP-induced spermatogenic cell apoptosis is not yet clear.

The interaction between Sertoli and spermatogenic cells is crucially important for successful spermatogenesis, because Sertoli cells form sites of attachment to spermatogenic cells. These Sertoli cells possess a highly organized and quite active cytoskeleton. The cytoskeleton consists of three major components, namely, microfilaments (actin), intermediate filaments and microtubules

(tubulin). In Sertoli cells, intermediate filaments are of vimentin type, with a molecular weight of 55–58 kDa (Franke et al., 1979). Vimentin filaments, formed by polymerization of 57 kDa vimentin monomers, surround the nucleus, give it the characteristic 'halo' appearance (Show et al., 2003), radiate outward to the cell periphery, and terminate near points of contact between Sertoli cell and adjacent cells. Vimentin filaments mediate the tight junction between neighbouring Sertoli cells, as well as the desmosome-like junction located between Sertoli cells and spermatogenic cells and the ectoplasmic specialization between Sertoli cells and more advanced spermatogenic cells. It has been suggested that vimentin filaments play a role in positioning the Sertoli cell nucleus and anchoring spermatogenic cells to the seminiferous epithelium (Amlani and Vogl, 1988), or act as a mediator of cell signal transduction between the plasma membrane and nucleus. Thus, they are essentially important for spermatogenesis (Aumuller et al., 1988, 1992). On the contrary, the collapse of vimentin filaments after xenobiotic treatment correlated with the loss of structural integrity of the seminiferous epithelium, along with spermatogenic cell apoptosis (Johnson et al., 1991; Richburg and Boekelheide, 1996; Dalgaard et al., 2001).

Phthalate esters disrupt Sertoli-spermatogenic cell contacts in post-natal Sertoli-spermatogenic cell co-cultures several hours after exposure (Gray and Beamand, 1984) and alter signalling modulated by follicle-stimulating hormone in cultured Sertoli cells (Heindel and Chapin, 1989; Grasso et al., 1993). In prepubertal rats, an acute exposure to MEHP resulted in collapsed Sertoli cell vimentin filaments and spermatogenic cell sloughing (Richburg and Boekelheide, 1996). Our previous study using an *in vitro* model, primary Sertoli cell culture, has also reported that MEHP disrupts vimentin filaments in mice Sertoli cells several hours after administration (Tay et al., 2007). Unfortunately, the mechanism underlying the cytotoxic effects of DBP on spermatogenic cell apoptosis, as well as the effects on Sertoli cell vimentin filaments, is not completely understood. Thus, the aim of this study was to examine a specific and early DBP-induced collapse of Sertoli cell vimentin filaments *in vivo* and *in vitro* and correlation between collapse of vimentin filaments and previously reported time course rates of spermatogenic cell apoptosis induced by a single DBP administration (Alam et al., 2010).

Materials and Methods

Animals and treatments

Male Sprague-Dawley (SD) rats (3-week-old) were purchased from Charles River Laboratories Japan (Tokyo, Japan). The rats were housed three to five per one plastic cage, maintained on a 12-h light/dark cycle at a constant temperature (22 ± 1°C) and humidity (45–70%), and provided water and rodent pellets (Oriental Yeast, Tokyo, Japan) *ad libitum*. Animals were maintained and handled humanely in accordance with the guideline of the animal experiments of the Institutional Animal Care and Use Committee (IACUC) of the University of Tokyo, Tokyo, Japan.

Three-week-old male rats ($n = 8$) were given a single oral administration of 500 mg/kg DBP in vehicle at a volume equal to 4 ml/kg. The vehicle was a mixture of 5% ethanol and 95% corn oil. Control animals received the same volume of vehicle. Rats were then killed under diethyl ether anaesthesia at 6 and 24 h after administration, and their testes were collected and subjected to histopathology.

The chosen dose of DBP was based on our earlier report in which a single administration of 500 mg/kg was sufficient for significantly increased number of spermatogenic cell apoptosis (Alam et al., 2010).

Sertoli cell culture and DBP treatment

Mixed cultures of Sertoli and spermatogenic cells were prepared from 3-week-old SD rats as described earlier (Worrell et al., 1989; Tay et al., 2007) with adaptations, and were maintained at 32°C in 25 cm^2 tissue culture flasks. In brief, testes were excised, decapsulated, cut into smaller pieces, and treated with 0.1% collagenase (Sigma, St. Louis, MO, USA). Single cells were obtained by gravity sedimentation and usage of 50% trypsin-EDTA (Gibco, Michele Serro, NY, USA). Cells were finally suspended at a concentration of 1×10^8 cell/ml and maintained for 24 h in Dulbecco's modified Eagle medium (Sigma) supplemented with 100 U/ml penicillin, 100 μg/ml streptomycin (Gibco), and 10% fetal bovine serum (Sigma). Thereafter, cells were maintained in serum-free medium, which was changed every 24 h. At 72 h, spermatogenic cells were removed by treatment with hypotonic Tris buffer (20 mM Tris–HCL, pH 7.4) for 5 min as described by Galdieri et al. (1981). The Sertoli cell-enriched cultures obtained were then maintained in serum-free medium for 24 h before being reseeded onto chamber slides. The samples were cultured for further 5 days. Subsequently, they were exposed to 0, 0.1, 1, and 100 nmol/ml DBP for 6 and 24 h. Some slides were stained with 1% toluidine blue for light microscopic observations, whereas the rest were used for vimentin immunohistochemical analysis.

Light microscopy

For histopathological observations (haematoxylin and eosin or immunohistochemical staining), under diethyl

ether anesthesia, rats were perfused with 10% neutrally buffered formalin for 30 min. Following perfusion, the testes were excised and immersed in the same fixative for 48 h. Then, the samples were washed in 0.1 M phosphate buffer solution for 3 h, dehydrated through a graded series of ethanol, cleared in xylene, and embedded in paraffin. The paraffin blocks were cut at 4 μm in thickness. The sections were then stained with Meyer's haematoxylin and eosin and/or periodic acid-Schiff (PAS)-haematoxylin. They were observed by light microscopy.

Transmission electron microscopy

For transmission electron microscopy, under diethyl ether anaesthesia, rats were perfused with 5% glutaraldehyde in 0.1 M phosphate buffer. Then, the testes were excised, immersed in the same fixative at 4°C for 3 h and post-fixed in 1% osmium tetroxide (OsO_4) at 4°C for 2 h. The samples were then dehydrated in a graded series of ethanol, infiltrated in propylene oxide, and embedded in Araldite M. Semi-thin sections were cut at about 1 μm in thickness, stained with 1% toluidine blue, and observed by light microscopy. Ultrathin sections were cut, and stained with uranyl acetate and lead citrate. In the DBP-treated rats, unique lesions were encountered at the light microscopic level at 24 h. Corresponding tissue sections from these animals, along with appropriate control sections, were examined using a JEM-1010 transmission electron microscope at 80 kV (JEOL, Ltd, Tokyo, Japan). Evaluation was limited to characterization of subtle lesions and abnormal cells, because quantitative analysis is impractical with transmission electron microscopy.

Immunohistochemistry

For vimentin immunohistochemistry on primary Sertoli cell cultures, a monoclonal anti-vimentin antibody (mouse immunoglobulin M [IgM] isotype, clone LN-6; Sigma) at a dilution 1:200 was used for staining vimentin in Sertoli cells. Slides were fixed in 10% neutrally buffered formalin for 20 min, rinsed in PBS, blocked with a TNB (0.1 M Tris–HSC, 0.15 M MaCl, 0.5% blocking reagent, pH 7.5) blocking buffer, supplied in tyramide signal amplification (TSA) Biotin System Kit (Perkin Elmer Life Sciences, Boston, MA, USA), and incubated at 4°C overnight with primary antibody. Thereafter, the sections were incubated with biotinylated goat anti-mouse IgG secondary antibody for 1–2 h at room temperature, followed by the ABC kit (Funakoshi, Tokyo, Japan). Immunoreaction was visualized with 0.05% diaminobenzidine tetrahydrochloride (DAB) (Wako, Tokyo, Japan) with H_2O_2 in PBS. The sections were lightly counterstained with haematoxylin. For a negative control, the incubation step with the primary antibody was omitted.

For another immunohistochemistry, the sections were deparaffinized, rinsed in PBS, rehydrated, and latter heated in 0.01 M citrate buffer (pH 6.0) for 10 min in a microwave to facilitate antigen retrieval. They were treated with 3% H_2O_2 for 30 min to eliminate endogenous peroxidase, blocked with a TNB blocking buffer, and incubated at 4°C overnight with primary antibody. A monoclonal antibody to vimentin was used at a dilution of 1:200, mouse monoclonal anti-α tubulin (Clone DM 1A, Sigma) was 1:200 and mouse monoclonal anti-actin antibody (Clone 1A4, Sigma) was 1:5000 dilution. Thereafter, protocols were similar as described above.

Results

Histopathology

Histopathology was evaluated using cross-sections of seminiferous tubules by light (haematoxylin–eosin or toluidine blue staining) and transmission electron microscopies. In haematoxylin and eosin stained sections, detachment of spermatogenic cells away from the basement membrane and sloughing of them into the lumen were observed in the DBP-treated group, compared with the control (Fig. 1a–c). In semi-thin sections stained with toluidine blue (Fig. 1d–f), degenerative spermatogenic cells were easily detected by their condensed nuclear chromatin, one of the hallmarks of apoptotic cell death. Degenerative spermatogenic cells were frequently observed in the DBP-treated group, compared with the control (Fig. 1d–f). A maximum number of degenerative spermatogenic cells were detected at 6 h after treatment (Fig. 1e). By careful observations, some nuclear chromatin condensed cells surrounded by an empty space were recognizable. They might fall away from their neighbours. In transmission electron microscopic observations, it was apparently distinguishable that the degenerative spermatogenic cells detached from their neighbours were surrounded by an empty space at 6 h after DBP treatment, whereas normal spermatogenic cells had a close contact with their neighbours in the control (Fig. 1g, h). These degenerative spermatogenic cells appeared to be apoptotic in nature based on break in DNA when being visualized by *in situ* terminal deoxynucleotidyl transferase-mediated digoxigenin-dUTP nick end-labeling (TUNEL) method (data not shown).

Vimentin staining

Vimentin filaments were visualized by immunohistochemistry (Fig. 2a–c). In Sertoli cells of the control, vimentin filaments could be seen as projections extending from the

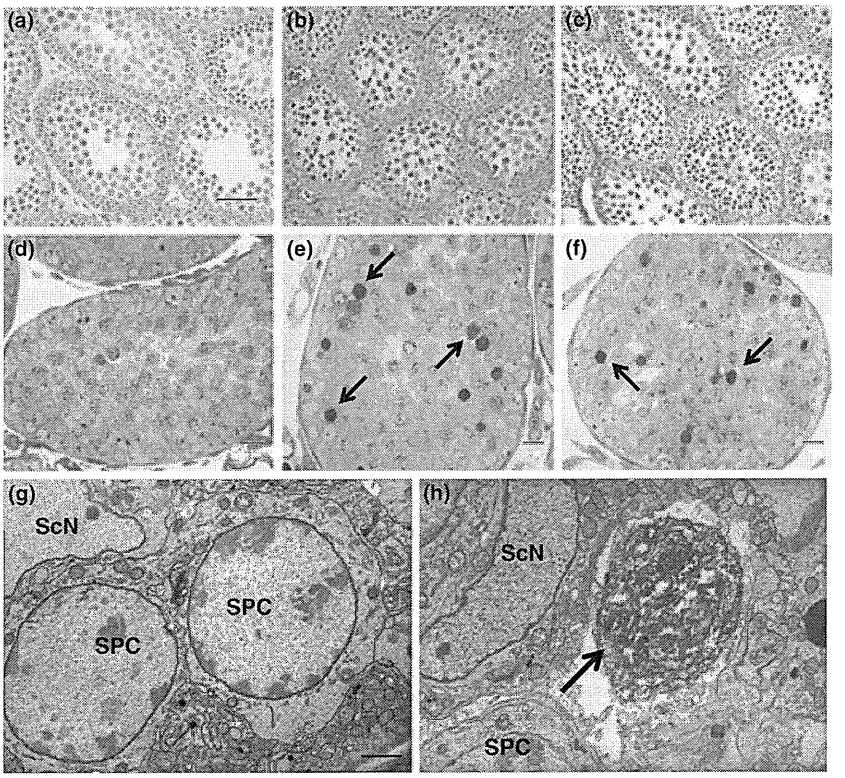

Fig. 1. Histological changes in testes after a single administration of 500 mg DBP/kg are shown. Haematoxylin and eosin staining sections (a–c), semi-thin sections stained with toluidine blue (d–f) and transmission electron micrographs (g–h). Control (a, d and g), at 6 h (b, e and h), and at 24 h (c and f) after treatment. Arrows indicate degenerative spermatogenic cells isolated by an empty space from their neighbours. ScN, Sertoli cell nucleus; SPC, spermatocyte. Scale bar, a–c = 50 μm, d–f = 30 μm, and g, h = 1 μm.

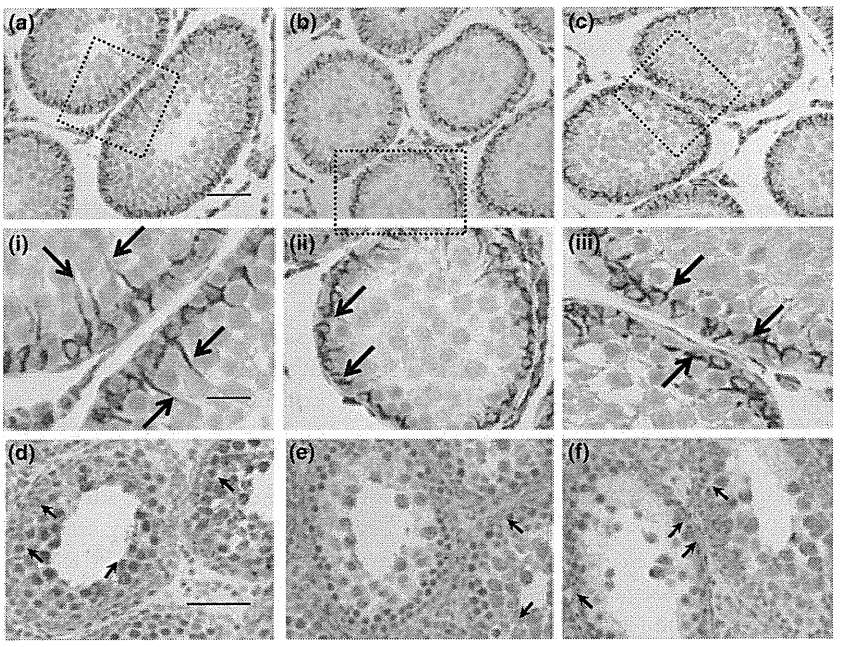

Fig. 2. Di(*n*-butyl) phthalate-induced cytoskeletal disruption in Sertoli cells is shown. Vimentin staining (a–c, i–iii) and actin staining (d–f). Control (a, i, d), at 6 h (b, ii, e), and at 24 h (c, iii, f) after treatment. Rectangles in a, b, and c are shown in i, ii, and iii at higher magnification, respectively. Note that in the control (a, i), vimentin filaments can be seen as projections extending from the perinuclear regions of Sertoli cell toward the lumen (arrows). Abundant apical extensions of vimentin filaments show collapsed and densely concentrated around the Sertoli cell nucleus (arrows) at 6 h (b, ii) and at 24 h (c, iii) after treatment. Actin (arrows) staining intensity is low in treated groups (e, f), compared with the control (d). Detachment and displacement of spermatogenic cells can also be seen in treated groups. Scale bar, a–c = 50 μm, i–iii, and d–f = 20 μm.

basal region towards the lumen (Fig. 2a, i). At 6 h after DBP administration, vimentin filaments showed shorter projections and concentrated near the basal region, while spermatogenic cells were detached away from the basement membrane and sloughed into the lumen (Fig. 2b, ii). At 24 h after treatment, a dramatic loss of vimentin filaments in apical extensions (Fig. 2c, iii) was detected, indicating the collapse of vimentin filaments in the DBP-treated rats.

To determine whether the effects of DBP were specific for Sertoli cell vimentin filaments, the staining pattern of α-tubulin was examined. The α-tubulin staining pattern was characterized by the long-defined tracts extending along the axis of the Sertoli cell. No difference was observed in distribution between the DBP-treated and control rats (data not shown). This finding demonstrated that DBP did not disrupt the Sertoli cell microtubule network. Actin staining in cross-sections of the control showed very strong in the basal region of Sertoli cells, probably corresponding to tight junctions and peripheral regions of spermatocytes (Fig. 2d), whereas the staining was weak in intensity in the DBP treated rats testes (Fig. 2e, f).

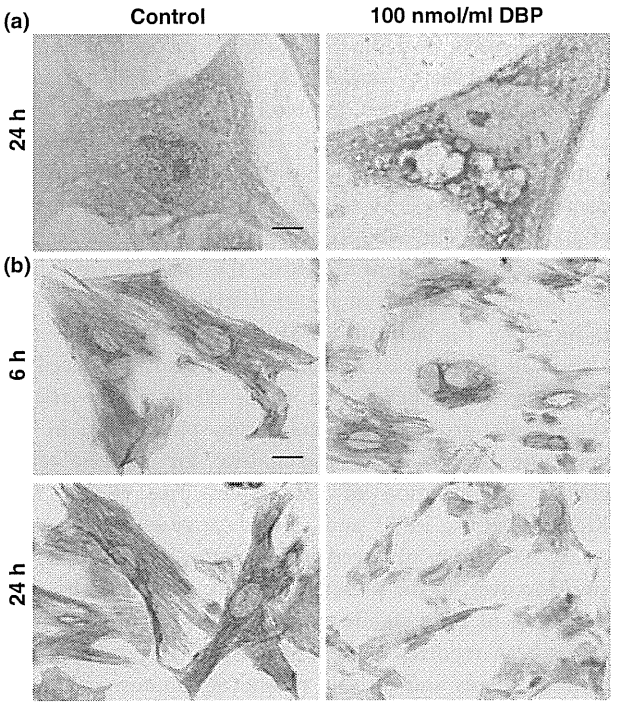

Fig. 3. Toluidine blue and vimentin staining in cultured Sertoli cells. At 24 h, 100 nmol/ml DBP-treated Sertoli cell shows severe vacuolation with multiple vacuoles, compared to vehicle-treated Sertoli cell (a). Vimentin filaments show severely collapsed and densely concentrated around the nucleus in 100 nmol/ml DBP-treated Sertoli cells at 6 and 24 h, compared to strong staining in the controls (b). Scale bar, a = 10 μm, b = 30 μm.

Primary Sertoli cell culture

Sertoli cells in culture treated with DBP and later stained with toluidine blue, showed the presence of vacuoles in the cytoplasm. The vacuoles were increased in number and size in time- and dose-dependant manners (data not shown). The maximum size and number of vacuoles were seen at highest dose (100 nmol/ml) for 24 h, compared with the control (Fig. 3a).

In order to clarify the vimentin expression in isolated Sertoli cells, we conducted anti-vimentin immunohistochemical staining in primary Sertoli cell cultures treated with DBP for 6 and 24 h. In the Sertoli cells control, vimentin filaments surrounded the Sertoli cell nucleus and radiated out from the nucleus to the cell periphery (Fig. 3b). Exposure to DBP caused a gradual collapse of vimentin filaments, and Sertoli cell conjunctions were detached. Thus, vimentin filaments were distributed only around the Sertoli cell nucleus in the treated groups, and gradually notable with increased concentrations of DBP. Vimentin expression was decreased with increased exposure time in 0.1 and 1 nmol/ml DBP treated groups (data not shown). Severe collapse of vimentin filaments was observed at 6 and 24 h in 100 nmol/ml treated groups, compared with the strong reaction noted in the control (Fig. 3b). Thus, *in vivo* and *in vitro* data clearly demonstrated that DBP exposure collapsed vimentin filaments in Sertoli cells.

Discussion

In earlier studies, rapid disruption of Sertoli cell-spermatogenic cell physical interactions, ultimately leading to detachment and sloughing of spermatogenic cells from the seminiferous epithelium, was observed after several Sertoli cell toxicants, including phthalate esters, administration (Creasy et al., 1987; Richburg and Boekelheide, 1996). The underlying mechanism for the detachment of spermatogenic cells away from the seminiferous epithelium induced by DBP has not yet been clarified. However, many researchers commonly believe that the Sertoli cell is the primary target of phthalate esters based upon Sertoli cell specific biochemical and morphological alterations after treatment (Creasy et al., 1983; Dostal et al., 1987; Lloyd and Foster, 1988; Boekelheide, 1993; Richburg and Boekelheide, 1996; Boekelheide et al., 2005). On this point, no data are available on DBP. Spermatogenic cell loss in the seminiferous epithelium was found to result from Sertoli cell dysfunction (Foster et al., 1982; Gray and Beamand, 1984). The Sertoli cell is responsible for orchestrating the differentiation of spermatogenic cells as well as providing nutritional and physiological supports (Aumuller et al., 1988, 1992).

In order to characterize the effects of DBP on Sertoli cells, we carried out two experiments: (1) *in vivo* experiment; a single administration of DBP to prepubertal rats to examine the early and specific effects of DBP on Sertoli cells-spermatogenic cells contact, (2) *In vitro* experiment; primary Sertoli cell cultures treated with DBP to examine the direct effect of DBP on morphology and collapse of vimentin filaments in isolated Sertoli cells. In *in vivo* observations, DBP-induced collapse of Sertoli cell vimentin filaments appears to be a reflection of detachment and displacement of spermatogenic cells away from basement membrane and sloughing of them into the lumen.

In cultured Sertoli cells stained with toluidine blue in the present study showed the presence of different-sized vacuoles. Higher concentration and longest exposure period of DBP revealed more dramatic morphological effects on Sertoli cells. It has been suggested that vacuolation in Sertoli cells is the earliest morphological sign of testicular injury, and the cardinal response is seen with many Sertoli cell toxicants (Creasy et al., 1987). In accordance with *in vivo* experiment, in *in vitro* experiment, we have also confirmed that the Sertoli cell cytoskeleton responds to DBP by exhibiting a marked collapse in vimentin filaments distribution in cultured Sertoli cells. Exposure to DBP collapses vimentin filaments, and then spermatogenic cell may detach from Sertoli cells in a dose-dependent manner. In the earlier reports, the collapse of Sertoli intermediate filaments has been observed in cryptorchid testes of immature rats *in vivo* (Wang et al., 2002; Kopecky et al., 2005); in such testes, immunohistochemical staining of vimentin filaments revealed loss of their extension and collapse at their perinuclear localization, coinciding with massive spermatogenic cell apoptosis. In addition, the break down of Sertoli cell intermediate filaments has also been reported in MEHP (Lloyd and Foster, 1988; Richburg and Boekelheide, 1996; Tay et al., 2007) or colchicine (Allard et al., 1993) treatment, resulting in loss of structural integrity of the seminiferous epithelium followed by spermatogenic cell apoptosis and sloughing. Similarly, alteration of Sertoli cell vimentin filaments distribution has been shown in 2,5-hexanedione (Hall et al., 1991) or fungicide benomyl (Hess and Nakai, 2000) administration and hormonal withdrawal (Show et al., 2003). Thus, the collapse of Sertoli cell vimentin filaments leads to detachment of spermatogenic cells from Sertoli cells, and that is the first step towards cell death. Since these vimentin-detached spermatogenic cells lost the support and nurture provided by Sertoli cells, they can no longer survive and will eventually undergo apoptosis after DBP (present study), MEHP or other Sertoli cells toxicants treatment (Richburg and Boekelheide, 1996; Tay et al., 2007), increased temperature (cryptorchidism) (Wang et al., 2002; Kopecky et al., 2005), and hormonal withdrawal (Show et al., 2003). However, it remains unclear, in all the instances, whether the loss of vimentin filaments structure is a cause of spermatogenic cell apoptosis after testicular toxicant insult, or is a secondary effect resulting from loss of spermatogenic cell adhesion that occurs by other undefined mechanism.

Caspases are key mediators of apoptosis. Two major pathways (intrinsic and extrinsic) are involved in the process of caspase activation and apoptosis in mammalian cells. The intrinsic pathway for apoptosis involves the release of cytochrome c from mitochondria, then auto-activation of initiator caspase-9, and subsequently proteolytic activity of executioner caspase-3, -6, and -7 (Cecconi, 1999; Hengartner, 2000; Newmeyer and Ferguson-Miller, 2003). The extrinsic pathway for apoptosis involves the binding of a death receptor (Fas), to its ligand, FasL (Krammer, 2000; Algeciras-Schimnich et al., 2002). The binding of FasL to Fas induces the recruitment of initiator caspase-8 or -10 via a series of interactions, and ultimately activates executioner caspase -3, -6, and -7 resulting in cellular disassembly (Hengartner, 2000; Krammer, 2000; Algeciras-Schimnich et al., 2002). Both pathways converge on effector caspase-3, -7, and -6, which drive the terminal events of apoptosis. Byun et al. (2001) showed *in vitro* that apoptosis induced by truncated/collapsed vimentin is dependent on caspases activity, notably effector caspases 3, 6, and 7, and they also reported that caspases inhibitors antagonize truncated vimentin-induced apoptosis. In addition, truncated vimentin has also been shown to be a substrate for proteolytic cleavage by the initiator caspase 9 (Nakanishi et al., 2001). Similarly, in Jurkat cells stably transfected with a caspase-resistant vimentin, the onset of condensation or fragmentation of nuclei delayed during apoptosis induced by Fas activation (Morishima, 1999), and this stable cell line showed resistance to apoptosis induced by oxidative stress (Belichenko et al., 2001). These results suggest that truncated vimentin may play a role in the apoptotic process as a prerequisite for morphological change. Participation of Fas system (Lee et al., 1997; Richburg et al., 1999) and cleaved caspases (Bissonnette et al., 2008) were observed in phthalates-induced apoptosis. Moreover, in the present study, we have also observed reduction of actin staining intensity after DBP treatment. It has been reported earlier that caspase cleavage disrupts actin filaments and directly promotes apoptosis (Brancolini et al., 1995; Kothakota et al., 1997). Thus, it seems that activation of caspases and/or Fas/FasL may cause truncation of Sertoli cell vimentin filaments or vise-versa, and subsequently may induce spermatogenic cell apoptosis after DBP administration to prepubertal rats. However, this does not preclude the possibility of other mechanism for this phenomenon. The observations

reported in this study may provide insights into the mechanisms that regulate spermatogenic cell apoptosis in toxicant-induced testicular injury.

Acknowledgements

This work was supported in part by Grants-in-Aid from the Ministry of Education, Culture, Sports, Science and Technology of Japan (to M. Kurohmaru).

Conflict of interest statement

None of the authors has a conflict of interest.

References

Alam, M. S., S. Ohsako, T. Matsuwaki, B. X. Zhu, N. Tsunekawa, Y. Kanai, H. Sone, C. Tohyama, and M. Kurohmaru, 2010: Induction of spermatogenic cell apoptosis in prepubertal rats testes irrespective of testicular steroidogenesis: a possible estrogenic effect of di(n-butyl) phthalate. Reproduction. **139**, 427–437.

Algeciras-Schimnich, A., L. Shen, B. C. Barnhart, A. E. Murmann, J. K. Burkhardt, and M. E. Peter, 2002: Molecular ordering of the initial signaling events of CD95. Mol. Cell. Biol. **22**, 207–220.

Allard, E. K., K. J. Johnson, and K. Boekelheide, 1993: Colchicine disrupts the cytoskeleton of rat testis seminiferous epithelium in a stage dependent manner. Biol. Reprod. **48**, 143–153.

Amlani, S., and A. W. Vogl, 1988: Changes in the distribution of microtubules and intermediate filaments in mammalian Sertoli cells during spermatogenesis. Anat. Rec. **220**, 143–160.

Aumuller, G., M. Steinbruck, W. Krause, and H. J. Wagner, 1988: Distribution of vimentin-type intermediate filaments in Sertoli cells of the human testis, normal and pathologic. Anat. Embryol. **172**, 129–136.

Aumuller, G., C. Schulze, and C. Viebahn, 1992: Intermediate filaments in Sertoli cells. Microsc. Res. Tech. **20**, 50–72.

Belichenko, I., M. Morishima, and D. Separovic, 2001: Caspase-resistant vimentin suppresses apoptosis after photodynamic treatment with a silicon phthalocyanine in Jurkat cells. Arch. Biochem. Biophys. **390**, 57–63.

Bissonnette, S. L., J. E. Teague, D. H. Sherr, and J. J. Schlezinger, 2008: An endogenous prostaglandin enhances environmental phthalate-induced apoptosis in bone marrow B cells: activation of distinct but overlapping pathways. J. Immunol. **181**, 1728–1736.

Boekelheide, K., 1993: Cell toxicants. In: The Sertoli Cell (L. D. Russell and M. D. Griswold eds). Florida: Cache River Press, pp. 551–575.

Boekelheide, K., K. K. Johnson, and J. H. Richburg, 2005: Sertoli cell toxicants. In: Sertoli Cell Biology (M. K. Skinner and M. D. Griswold eds). San Diego: Elsevier Academic Press, pp. 345–382.

Brancolini, C., M. Benedetti, and C. Schneider, 1995: Microfilament reorganization during apoptosis: the role of Gas2, a possible substrate for ICE-like proteases. EMBO J. **14**, 5179–5190.

Byun, Y., F. Chen, R. Chang, M. Trivedi, K. J. Green, and V. L. Cryns, 2001: Caspase cleavage of vimentin disrupts intermediate filaments and promotes apoptosis. Cell Death Differ. **8**, 443–450.

Cecconi, F., 1999: Apaf1 and the apoptotic machinery. Cell Death Differ. **6**, 1087–1098.

Creasy, D. M., J. R. Foster, and P. M. Foster, 1983: The morphological development of di-N-pentyl phthalate induced testicular atrophy in the rat. J. Pathol. **139**, 309–321.

Creasy, D. M., L. M. Beech, T. J. B. Gray, and W. H. Butler, 1987: The ultrastructural effects of di-n-pentyl phthalate on the testis of the mature rat. Exp. Mol. Pathol. **46**, 357–371.

Dalgaard, M., A. Hossaini, K. S. Hougaard, U. Hass, and O. Ladefoged, 2001: Developmental toxicity of toluence in male rats: effects on semen quality, testis morphology, and apoptotic neurogeneration. Arch. Toxicol. **75**, 103–109.

Dostal, L. A., R. E. Chapin, S. A. Stefanski, M. W. Harris, and B. A. Schwetz, 1987: Testicular toxicity and reduced Sertoli cell numbers in neonatal rats by di(2-ethylhexyl)phthalate and the recovery of fertility as adults. Toxicol. Appl. Pharmacol. **95**, 104–121.

Foster, P. M. D., J. R. Foster, M. W. Cook, L. V. Thomas, and S. D. Gangolli, 1982: Changes in ultrastructure and cytochemical localization of zinc in rat testis following the administration of di-n-pentyl phthalate. Toxicol. Appl. Pharmacol. **63**, 120–132.

Franke, W. W., C. Grund, and E. Schmid, 1979: Intermediate-sized filaments present in Sertoli cells are of the vimentin type. Eur. J. Cell Biol. **19**, 269–275.

Galdieri, M., E. Ziparo, F. Palombi, M. A. Russo, and M. Stefanini, 1981: Pure Sertoli cell cultures: a new model for the study of somatic-germ cell interactions. J. Androl. **2**, 249–254.

Grasso, P., J. J. Heindel, C. J. Powell, and L. E. . Reichert Jr, 1993: Effects of mono(2-ethylhexyl) phthalate, a testicular toxicant, on follicle-stimulating hormone binding to membranes from cultured rat Sertoli cells. Biol. Reprod. **48**, 454–459.

Gray, T. J. B., and J. A. Beamand, 1984: Effects of some phthalate esters and other testicular toxins on primary cultures of testicular cells. Food Chem. Toxicol. **22**, 123–131.

Hall, E. S., J. Eveleth, and K. Boekelheide, 1991: 2,5-Hexanedione exposure alters the rat Sertoli cell cytoskeleton. II. Intermediate filaments and actin. Toxicol. Appl. Pharmacol. **111**, 443–453.

Heindel, J. J., and R. E. Chapin, 1989: Inhibition of FSH-stimulated cAMP accumulation by mono(2-ethylhexyl) phthalate in primary rat Sertoli cell cultures. Toxicol. Appl. Pharmacol. **97**, 377–385.

Hengartner, M. O., 2000: The biochemistry of apoptosis. Nature **407**, 770–776.

Hess, R. A., and M. Nakai, 2000: Histopathology of the male reproductive system induced by the fungicide benomyl. Histol. Histopathol. **15**, 207–224.

Johnson, K. J., E. S. Hall, and K. Boekelheide, 1991: 2,5-Hexanedione exposure alters the rat Sertoli cell cytoskeleton. I. Microtubules and seminiferous tubule fluid secretion. Toxicol. Appl. Pharmacol. **111**, 432–442.

Kopecky, M., V. Semecky, and P. Nachtigal, 2005: Vimentin expression during altered spermatogenesis in rats. Acta Histochem. **107**, 279–289.

Kothakota, S., T. Azuma, C. Reinhard, A. Klippel, J. Tang, K. Chu, T. J. McGarry, M. W. Kirschner, K. Koths, D. J. Kwiatkowski, and L. T. Williams, 1997: Caspase-3-generated fragment of gelsolin: effector of morphological change in apoptosis. Science **278**, 294–298.

Krammer, P. H., 2000: CD95's deadly mission in the immune system. Nature **407**, 789–795.

Lee, J., J. H. Richburg, S. C. Younkin, and K. Boekelheide, 1997: The Fas system is a key regulator of germ cell apoptosis in the testis. Endocrinology **138**, 2081–2088.

Lloyd, S. C., and P. M. Foster, 1988: Effect of mono-(2-ethylhexyl) phthalate on follicle-stimulating hormone responsiveness of cultured rat Sertoli cells. Toxicol. Appl. Pharmacol. **95**, 484–489.

Morishima, N., 1999: Changes in nuclear morphology during apoptosis correlate with vimentin cleavage by different caspases located either upstream or downstream of Bcl-2 action. Genes Cells **4**, 401–414.

Nakanishi, K., M. Maruyama, T. Shibata, and N. Morishima, 2001: Identification of a caspase-9 substrate and detection of its cleavage in programmed cell death during mouse development. J. Biol. Chem. **276**, 41237–41244.

Newmeyer, D. D., and S. Ferguson-Miller, 2003: Mitochondria: releasing power for life and unleashing the machineries of death. Cell **112**, 481–490.

Oishi, S., and S. Hiraga, 1980: Testicular atrophy induced by phthalic acid monoesters: effects of zinc and testosterone concentrations. Toxicology **15**, 197–202.

Richburg, J. H., and K. Boekelheide, 1996: Mono-(2-ethylhexyl) phthalate rapidly alters both Sertoli cell vimentin filaments and germ cell apoptosis in young rat testes. Toxicol. Appl. Pharmacol. **137**, 42–50.

Richburg, J. H., A. Nanez, and H. Gao, 1999: Participation of the Fas-signaling system in the initiation of germ cell apoptosis in young rat testes after exposure to mono-(2-ethylhexyl) phthalate. Toxicol. Appl. Pharmacol. **160**, 271–278.

Show, M. D., M. D. Anway, J. S. Folmer, and B. R. Zirkin, 2003: Reduced intratesticular testosterone concentration alters the polymerization state of the Sertoli cell intermediate filament cytoskeleton by degradation of vimentin. Endocrinology **144**, 5530–5536.

Tay, W. T., B. B. Andrina, M. Ishii, N. Tsunekawa, Y. Kanai, and M. Kurohmaru, 2007: Disapperance of vimentin in Sertoli cells: A mono(2-ethylhexyl) phthalate effect. Int. J. Toxicol. **26**, 289–295.

Wang, Z. Q., Y. Watabane, A. Toki, and T. Itano, 2002: Altered distribution of Sertoli cell vimentin and increase dapoptosis in cryptorchid rats. J. Pediatr. Surg. **37**, 648–652.

Worrell, N. R., W. M. Cook, C. A. Thompson, and T. J. B. Gray, 1989: Effect of mono-(2-ethylhexyl) phthalate on the metabolism of energy-yielding substrates in rat Sertoli cell-enriched cultures. Toxicol. In Vitro **3**, 77–81.

BIOLOGY OF REPRODUCTION **82,** 636–643 (2010)
Published online before print 9 December 2009.
DOI 10.1095/biolreprod.109.080812

Comparative Contribution of the Aryl Hydrocarbon Receptor Gene to Perinatal Stage Development and Dioxin-Induced Toxicity Between the Urogenital Complex and Testis in the Mouse[1]

Seiichiroh Ohsako,[2,7] Noriho Fukuzawa,[3,8] Ryuta Ishimura,[4,8] Takashige Kawakami,[5,8] Qing Wu,[6,8] Reiko Nagano,[9] Hiroko Zaha,[9] Hideko Sone,[9] Junzo Yonemoto,[9] and Chiharu Tohyama[7]

Division of Environmental Health Sciences,[7] Center for Disease Biology and Integrative Medicine, Graduate School of Medicine, The University of Tokyo, Tokyo, Japan
Environmental Health Sciences Division[8] and Research Center for Environmental Risk,[9] National Institute for Environmental Studies, Ibaraki, Japan

ABSTRACT

TCDD (2,3,7,8-tetrachlorodebenzo-*p*-dioxin) requires the presence of the aryl hydrocarbon receptor (*Ahr*) gene for its toxic effects, such as reproductive disorders in male offspring of maternally exposed rats and mice. To study the involvement of the *Ahr* gene in producing the toxic phenotype with respect to testicular development, we administered a relatively high dose of TCDD to mice with three different maternally derived *Ahr* genotypic traits, and then compared several *Ahr*-dependent alterations among male reproductive systems on Postnatal Day 14. Reduction in anogenital distance and expression of prostatic epithelial genes in the urogenital complex (UGC) were detected in $Ahr^{+/+}$ and $Ahr^{+/-}$ mice exposed to TCDD, whereas no difference was observed in $Ahr^{-/-}$ mice. In situ hybridization revealed the absence of probasin mRNA expression in the prostate epithelium, despite the obvious development of prostatic lobes in TCDD-exposed mice. In contrast to obvious prostatic dysfunction and induction of cytochrome P450 (CYP) family genes in the UGC by TCDD, no alterations in testicular functions were observed in germ cell/Sertoli cell/interstitial cell marker gene expression or CYP family induction. No histopathological changes were observed among the three genotypes and between control and TCDD-exposed mice. Therefore, mouse external genitalia and prostatic development are much more sensitive to TCDD treatment than testis. Further, the *Ahr* gene, analyzed in this study, does not significantly contribute to testicular function during perinatal and immature stages, and the developing mouse testis appears to be quite resistant to TCDD exposure.

aryl hydrocarbon receptor, developmental biology, dioxin, knockout mouse, prostate, spermatogenesis, testis, toxicology

INTRODUCTION

TCDD (2,3,7,8-tetrachlorodebenzo-*p*-dioxin) is an extremely potent xenobiotic chemical. Maternal exposure to TCDD induces a wide range of physiological alterations and toxicities in the fetus and pups of laboratory animals and perhaps in humans [1]. TCDD induces various toxicological endpoints in male reproductive organs, such as decreased size of sex-accessory glands and reduced sperm counts in testis, epididymis, and ejaculate [2–10]. Although male rat and mouse offspring exposed to TCDD in utero can produce testicular androgen normally, the androgen responsiveness of the ventral prostate is lowered by unknown mechanisms of TCDD [9–12].

Interestingly, the effects of TCDD on testicular development and perinatal stage spermatogenesis are still unclear because the results are contradictory [2–10]. Some studies on testicular development that used conventional experimental animals reported the presence of slight reductions in testicular weight, daily sperm production, and steroidogenesis [2–5]. On the other hand, clear negative data concerning the TCDD effect on testicular development were presented in many other papers [7–10]. Taken together, the impairment in prostate development by in utero TCDD exposure appears to occur in many mammals, including rats and mice, but it is not understood whether or how susceptible the testicular development and perinatal stage spermatogenesis is to the TCDD exposure.

The aryl hydrocarbon receptor (AHR) is a ligand-activated transcription factor that mostly mediates inductions of drug-metabolizing enzymes such as members of the CYP1A family, and it appears to act as a sensor for environmental contaminants such as dioxins and polyaromatic hydrocarbons [13, 14]. Experimental studies with *Ahr* gene knockout mice have already revealed that AHR plays an essential role in the occurrence of multiple TCDD-induced adverse effects, including teratogenic cleft palate and hydronephrosis [15, 16]. Reproductive disorders, such as prostatic growth impairment in male offspring following maternal exposure to TCDD, were also shown to be dependent on the *Ahr* gene [17].

Some evidence also suggested that AHR was involved in developmental signaling in the immune and hepatic systems [18, 19]. In analyses using *Ahr*-null female mice, AHR was

[1]Supported, in part, by the Environmental Technology Development Fund to S.O. and H.S. and the Risk Assessment of Dioxins Fund to C.T. from the Ministry of the Environment, Japan, and by grants from CREST, JST, Japan, to C.T.
[2]Correspondence: Seiichiroh Ohsako, Division of Environmental Health Sciences, Center for Disease Biology and Integrative Medicine, Graduate School of Medicine, The University of Tokyo, 7-3-1 Hongo, Bunkyo-ku, Tokyo 113-8654. FAX: 81 3 5841 1434;
e-mail: ohsako@m.u-tokyo.ac.jp
[3]Current address: Research Institute of Genome-based Biofactory, AIST, 2-17-2–1 Tsukisamu-higashi, Sapporo, Hokkaido 062-8517, Japan.
[4]Current address: The Jackson Laboratory, 600 Main St., Bar Harbor, ME 04609.
[5]Current address: School of Pharmaceutical Sciences, Tokushima-Bunri University, Tokushima 770-8514, Japan.
[6]Current address: School of Public Health, Fudan University, Shanghai 200032, China.

Received: 13 August 2009.
First decision: 2 September 2009.
Accepted: 17 November 2009.

eISSN: 1529-7268 http://www.biolreprod.org
ISSN: 0006-3363

also required for normal ovarian germ cell dynamics, based on the observation that numbers of nonatretic primordial, primary, and small preantral follicles in ovaries of *Ahr*-null females at early postpartum stages were higher than those in wild-type mice [20–22]. Moreover, AHR cooperates with an orphan nuclear receptor, NR5A1 (also known as Ad4BP/SF-1), to activate P450 aromatase (CYP19) gene transcription in ovarian granulosa cells and modulate endogenous estrogen production in the female reproductive cycle [23]. AHR is also expressed in interstitial cells and male germ cells at specific stages [24]. More recently, AHR has been demonstrated to have a ubiquitin ligase activity, which enhances the degradation of estrogen and androgen receptors, suggesting that AHR may modulate androgen sensitivity in normal development [25]. To date, the possible involvement of AHR in testicular development during immature stages using AHR agonist administration or *Ahr*-null male mice has not been addressed.

To the best of our knowledge, this is the first study that used *Ahr*-null mice to investigate the involvement of the *Ahr* gene in early stages of testicular development and to assess the differences in susceptibility to in utero TCDD exposure between prostate and testicular development.

MATERIALS AND METHODS

Materials

TCDD was purchased from Cambridge Isotope Laboratory (Andover, MA). The purity was higher than 99.5%. Corn oil for dissolving TCDD or the control vehicle was obtained from Sigma-Aldrich (St. Louis, MO). TRIzol reagent, SuperScript III RNase H- Reverse Transcriptase, and oligo(dT)12–18 primer were purchased from Invitrogen (Carlsbad, CA). SYBR Premix Ex Taq (Perfect Real Time) was purchased from TAKARA BIO, Inc. (Otsu, Japan). The plasmid pGEM-TEasy vector was obtained from Promega Corp. (Madison, WI).

Animals and TCDD Administration

Ahr knockout mice were kindly provided by Dr. Yoshiaki Fujii-Kuriyama (Center for Tsukuba Advanced Research Alliance and Institute of Basic Medical Sciences, University of Tsukuba) [15]. They were bred in our own facility at the National Institute for Environmental Studies (NIES). All described procedures were approved by the NIES Institutional Animal Care and Use Committee and were performed in accordance with the Guidelines for Animal Experiments at the NIES. They were maintained in a controlled environment of temperature 24 ± 1°C, humidity 45 ± 5%, and a 12L:12D cycle and were given food and distilled water ad libitum. *Ahr* heterozygous male mice were back-crossed with wild-type female C57BL/6J mice (CLEA Japan, Tokyo, Japan) six times, and heterozygous offspring of both sexes were used in this study. The heterozygous female mice (7- to 10-wk-old) were mated 1:1 with the heterozygous males overnight, and the females that had a vaginal plug on the following morning were designated as being pregnant at Gestational Day 0 (GD0). Dams were housed individually in clear plastic cages with heat-treated wood chips as bedding. On GD13, pregnant mice were given a single dose of TCDD orally (10 μg/kg body weight, close to a lethal dose for a C57BL/6J fetus) or an equivalent volume of vehicle (95% corn oil, 4% n-nonane; 5 ml/kg) as control. Male pups were killed under diethyl ether anesthesia on Postnatal Day 14 (PND14).

Sample Collection

On PND14, immediately before euthanization, the anogenital distance, determined by the length from the base of the genital tubercle to the anterior edge of the anus, was measured with a digital caliper. We also measured the crown-anal length (the distance between the nose and anterior edge of the anus). The testis and epididymis on both sides were excised from the abdomen, and the surrounding adipose tissue was carefully removed. After removing urine from the bladder, the deferent ducts were cut at the base of the bladder. The urogenital complex (UGC), which is a small mass comprising all the lobes of the prostate and seminal vesicle, was then collected by cutting the anterior end of the urethra. All tissue samples were frozen in liquid nitrogen immediately after dissection and kept at −80°C until RNA extraction.

Real-Time RT-PCR

The protocols for real-time RT-PCR quantifications were described previously [26]. Briefly, total RNA was extracted from the UGC (n = 5) and testis (n = 3) using TRIzol reagent. RNA samples were reverse-transcribed with SuperScript III reverse transcriptase and oligo(dT)12–18 primer. Nineteen genes examined in this study: aryl hydrocarbon receptor (*Ahr*), cytochrome P450 1A1 (*Cyp1a1*), cytochrome P450 1A2 (*Cyp1a2*), cytochrome P450 1B1 (*Cyp1b1*), androgen receptor (*Ar*), steroid 5α-reductase type 1 (*Srd5a1*), steroid 5α-reductase type 2 (*Srd5a2*), probasin (*Pbsn*), Mp25 (*Sbp*), PSP94 (*Msmb*), calnexin-t (*Clgn*), Hsp70.2 (*Hspa2*), androgen-binding protein (*Shbg*), cytochrome P450 side chain cleavage (*Cyp11a1*), cytochrome P450 17α/C_{17-20} lyase (*Cyp17a1*), 3β-hydroxysteroid dehydrogenase type I (*Hsd3b1*), 3α-hydroxysteroid dehydrogenase type I (*Akr1c4*), 17β-hydroxysteroid dehydrogenase type III (*Hsd17b3*), and cyclophilin B (*Ppib*). All primer sets are shown in Supplemental Table S1 (available online at www.biolreprod.org). For the real-time RT-PCR, target genes were amplified with SYBR Premix Ex Taq (Perfect Real Time) system by using a LightCycler (Roche, Manheim, Germany). The relative expression level was calculated by normalizing with the average value of each control wild-type ($Ahr^{+/+}$) group. To determine the sequences, the PCR product for each gene was subcloned into pGEM-TEasy vectors or directly sequenced by the dideoxynucleotide chain termination method using the ABI Prism BigDye terminator cycle sequencing kit (PE-Biosystems, Foster City, CA).

In Situ Hybridization

Mouse probasin mRNA was detected in the UGC specimens by in situ hybridization. The UGCs were fixed with neutralized formalin for 48 h, embedded in paraffin, and then cut into 4-μm sections. A template was amplified from the pGEM-TEasy vector inserted with a 377-bp probasin (*Pbsn*) RT-PCR fragment by T7 and SP6 primers to generate sense and antisense transcripts. Digoxigenin-labeled riboprobes were used, and the hybridization was performed using an automated in situ hybridization instrument Gen II (Ventana Medical System, Tucson, AZ). Detection and counterstaining were done with the BlueMap Kit (Ventana Medical System) and Nuclear Fast Red (Sigma-Aldrich).

Immunohistochemistry

Anti-calnexin-t (CLGN), a male germ cell developmental stage-specific protein, was immunostained by the method described previously [27]. Briefly, testes (n = 3; left side) were fixed with Bouin solution and embedded in paraffin. Two different cross-sectional regions (4-μm thickness) from one testis were obtained (six sections from each group). Deparaffinized sections were incubated with anti-mouse calnexin-t antibody, followed by incubation with peroxidase-conjugated goat anti-mouse or rabbit IgG. After washing with PBS, immunoreactivity was detected with diaminobenzidine, followed by hematoxylin counterstaining. Morphometric measurement of the amount of CLGN-positive germ cells was carried out using AxioVision version 4.5 software (Carl Zeiss Co., Ltd., Oberkochen, Germany). The total area of seminiferous tubules within the 1-mm^2 area of the cross-sections from each genotype and treatment group was traced and summed. Then, the CLGN-positive cell numbers were counted and divided by the total area traced for the seminiferous tubules.

Testosterone Assay

Testicular testosterone levels were determined by the enzyme immunoassay (EIA) Kit (Cayman Chemical Co., Ann Arbor, MI). The frozen testis was homogenized in PBS, and the protein concentration was measured by the BCA Protein Assay Kit (Pierce Biotechnology, Inc., Rockford, IL). The homogenate was then extracted with diethyl ether, and the ether phase was air-dried. The dried lipophilic substances were resuspended in the appropriate volume of EIA buffer, and the measurements were done according to the manufacturer's instructions.

Statistical Analysis

For statistical analysis, StatView for Windows version 5.0 (SAS Institute, Cary, NC) was used. All data were expressed relative to the means of the control groups. All results are represented as the mean ± SE. Two-way ANOVA was used for comparison of a given parameter among three control groups ($Ahr^{+/+}$, $Ahr^{+/-}$, $Ahr^{-/-}$), followed by the Fisher PLSD post hoc test. $P < 0.05$ was considered significant.

TABLE 1. Reproductive outcomes of male mice exposed to TCDD in utero.[a]

Parameter	Genotype		
	$Ahr^{+/+}$	$Ahr^{+/-}$	$Ahr^{-/-}$
No. of male pups			
Control (n)[b,c]	17 (1.70)	14 (1.40)	6 (0.60)
TCDD (n)[b,d]	6 (0.40)	16 (1.07)	9 (0.60)
Body weight (g)			
Control	6.82 ± 0.41	7.16 ± 0.23	6.04 ± 0.73
TCDD	5.49 ± 0.59	6.59 ± 0.55	7.55 ± 0.27
Crown-anal length (mm)			
Control	54.1 ± 1.2	55.7 ± 0.9	53.0 ± 2.2
TCDD	50.4 ± 2.0	53.1 ± 2.0	56.3 ± 0.9
Anogenital distance (mm)			
Control	3.82 ± 0.11	4.05 ± 0.19	3.66 ± 0.31
TCDD	3.19 ± 0.28*	3.27 ± 0.12**	3.33 ± 0.09
Testicular testosterone level (pg/mg protein)			
Control	140 ± 72 (n = 8)	173 ± 112 (n = 8)	141 ± 86 (n = 5)
TCDD	179 ± 73 (n = 5)	124 ± 33 (n = 8)	197 ± 126 (n = 5)

[a] Data are expressed as means ± SEM, and significant differences were analyzed with ANOVA followed by Fisher PLSD test (versus control of the same genotype, $*P < 0.05$, $**P < 0.01$).
[b] n = The number of male pups per litter.
[c] The number of dams = 10.
[d] The number of dams = 15.

RESULTS

Reproductive Outcome

The number, body weight, and crown-anal length of male pups in each genotype on PND14 are represented in Table 1. There were no statistically significant differences in body weight or crown-anal length among the three genotypes, or between control and TCDD-exposed groups. The number of $Ahr^{+/+}$ male pups exposed to TCDD was only six, which was much lower than the number of control pups, probably due to the fetal death by TCDD exposure in this genotype. Anogenital distance of $Ahr^{+/+}$ and $Ahr^{+/-}$ male pups in the TCDD-exposed groups was significantly reduced compared to control groups ($P = 0.016$ and $P = 0.001$, respectively). In contrast, the anogenital distance of $Ahr^{-/-}$ mice was not significantly different between TCDD-exposed and control mice. ANOVA did not reveal any significant differences in the mean anogenital distance among the three genotypes.

Gene Expressions in UGC

Quantitative RT-PCR analysis of the UGC on PND14 showed that *Ahr* mRNA was detected in $Ahr^{+/+}$ and $Ahr^{+/-}$ mice but not in the $Ahr^{-/-}$ mice. The expression level in the $Ahr^{+/+}$ group was 2-fold higher than that in the $Ahr^{+/-}$ mice, suggesting *Ahr* is transcribed from both alleles in the wild-type mice (Fig. 1). *Cyp1a1*, *Cyp1a2*, and *Cyp1b1* mRNAs, biomarkers of dioxin exposure, were not induced by TCDD

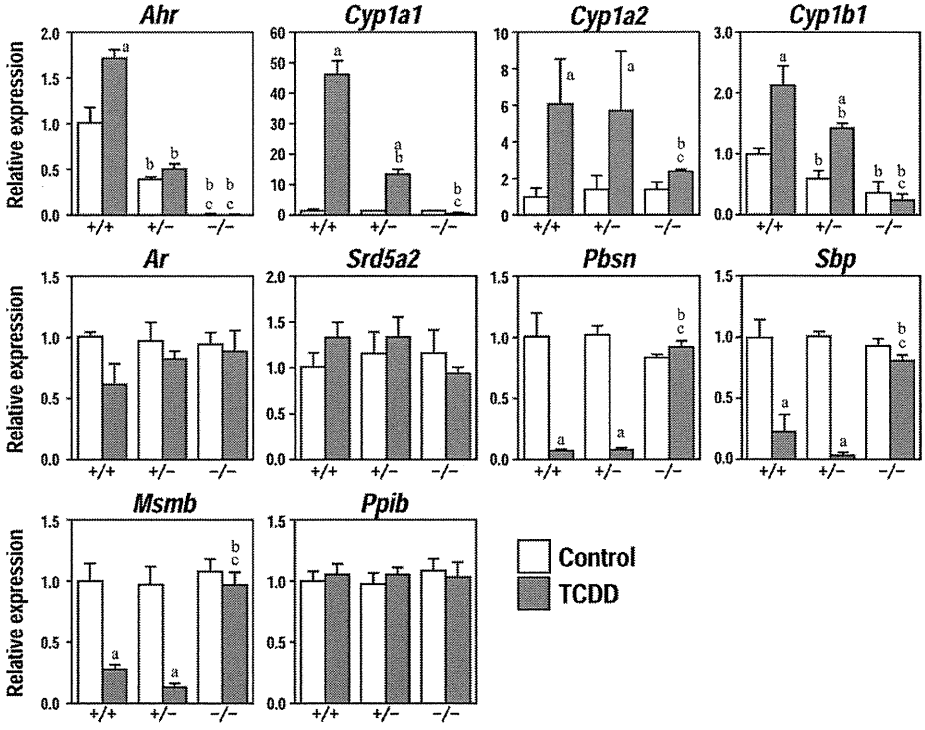

FIG. 1. Quantitative RT-PCR analysis of gene expressions in the urogenital complex of male mouse offspring of three *Ahr* genotypes ($Ahr^{+/+}$, $Ahr^{+/-}$, and $Ahr^{-/-}$) on PND14 with or without TCDD exposure in utero. The values are expressed as mean ± SE for three samples from each group. Note that in utero and lactational exposure to TCDD significantly upregulated *Cyp1a1* and *Cyp1b1* in $Ahr^{+/+}$ and $Ahr^{+/-}$ mice, but not in $Ahr^{-/-}$ mice and that it completely suppressed mRNA expression of the prostatic secretory protein markers *Pbsn*, *Sbp*, and *Msmb* in $Ahr^{+/+}$ and $Ahr^{+/-}$ mice. Significant differences were analyzed with ANOVA followed by the Fisher PLSD test (a, versus control of the same genotype; b, versus the same treatment of wild type; c, versus the same treatment of heterozygous; $P < 0.05$).

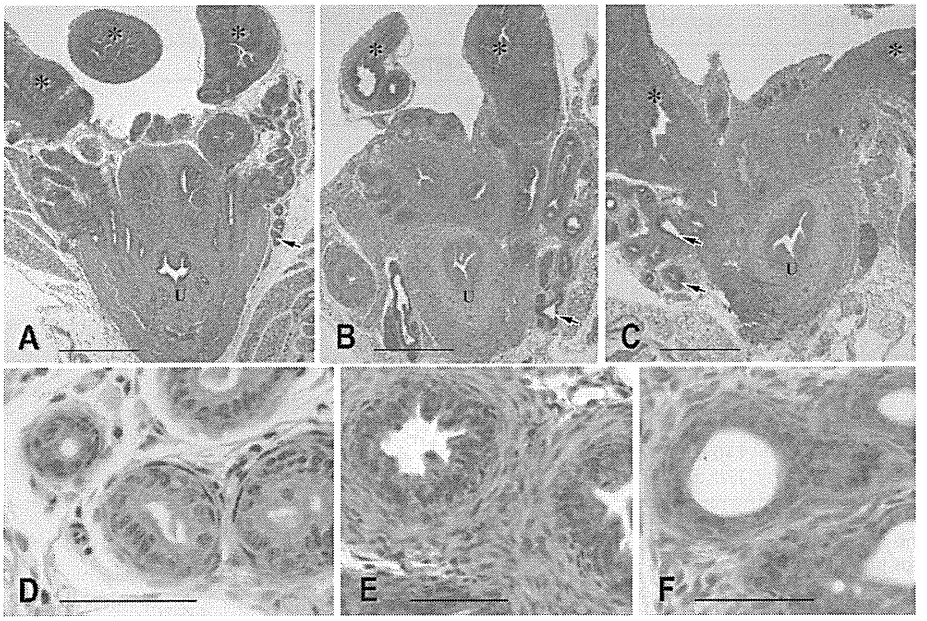

FIG. 2. Histological examinations of the UGC in male mouse pups on PND14. Hematoxylin-eosin staining of $Ahr^{+/+}$ UGCs (**A** and **D**, control; **B**, **C**, **E**, and **F**, TCDD-exposed). Note that control mice had well-developed prostatic lobes on PND14 (**A**). Fewer layers of epithelial cells and increased cell numbers in mesenchymal cells were observed in the dorsolateral prostate lobe of TCDD-exposed animals compared to controls (**E** and **F**). Asterisks, seminal vesicle; arrows, dorsolateral prostate; U, urethra. Bars = 500 μm (**A**, **B**, and **C**), 50 μm (**D**, **E**, and **F**).

in the $Ahr^{-/-}$ mice, but were significantly upregulated in $Ahr^{+/+}$ and $Ahr^{+/-}$ mice. In $Ahr^{+/+}$ and $Ahr^{+/-}$ mice, the *Cyp1b1* expression level in the TCDD-exposed group was higher than that in the control group (Fig. 1). Although a slight decrease of *Ar* mRNA was seen in the $Ahr^{+/+}$ mice (TCDD exposed), we did not detect any significant change in *Ar* and *Srd5a2* mRNA levels among the three TCDD-exposed genotypes. *Pbsn* (dorsolateral), *Sbp* (ventral), and *Msmb* (lateral) were used to investigate functional cytodifferentiation levels of each prostatic epithelia, as reported by others [28]. These three prostate markers were expressed in the control UGCs on PND14. They were barely detectable in TCDD-exposed $Ahr^{+/+}$ and $Ahr^{+/-}$ mice, while TCDD-exposed $Ahr^{-/-}$ mice had quantities of these three marker mRNAs that were very similar to control mice (Fig. 1).

Histopathology of the Urogenital Complex

Prostatic lobes were found to be well developed in the control animals (Fig. 2, A and D). In the TCDD-exposed $Ahr^{+/+}$ animals, the prostatic lobes with existing epithelial layers were clearly observed (Fig. 2, B, C, E, and F). In situ hybridization analysis of the tissue section adjacent to the sections used for histopathological examinations revealed that epithelial cells of dorsolateral prostate lobes had *Pbsn* mRNA signals (Fig. 3A). In accordance with the RT-PCR data, no signals were detected in the epithelia of TCDD-exposed dorsolateral prostates (Fig. 3C).

Gene Expressions in Testis

Consistent with the analysis of UGC (Fig. 1), the expression of *Ahr* mRNA was not detected in the $Ahr^{-/-}$ testis, whereas the *Ahr* expression level was 2-fold higher in the $Ahr^{+/+}$ than in the $Ahr^{+/-}$ mice. No differences were detected in *Ar* mRNA levels (Fig. 4). Among the three CYP1 genes tested, *Cyp1a1* mRNA was not detected in any of the *Ahr* genotypes (data not shown). Although *Cyp1a2* and *Cyp1b1* mRNA was detected in the testis, there were no statistically significant differences among the three genotypes and between the control and TCDD-exposed testes (Fig. 4). The mRNA of *CLGN* and *Hspa2*, male germ cell-specific markers expressed in the pachytene stage of spermatocytes [29, 30], was observed at the same levels among the three genotypes, regardless of TCDD exposure (Fig. 4). No difference was observed in the expression level of *Shbg*, a protein secreted from Sertoli cells [31]. RNA expression levels of four steroidogenic enzyme genes for testosterone synthesis, *Cyp11a1*, *Cyp17a1*, *Hsd3b1*, and *Hsd17b3*, were not affected in the three genotypes under the TCDD dosing regimen used (Fig. 4). Consistently, intratesticular testosterone levels in all genotypes and TCDD-exposed animals were not changed among the three genotypes, regardless of TCDD exposure (Table 1). Additionally the mRNA of *Akr1c4* and *Srd5a1* enzymes for synthesis of 5α-androstane-3α, 17β-diol, the major form of testicular androgen in immature mice [32], was not altered by TCDD exposure and showed no differences among the three genotypes in the testes (Fig. 4).

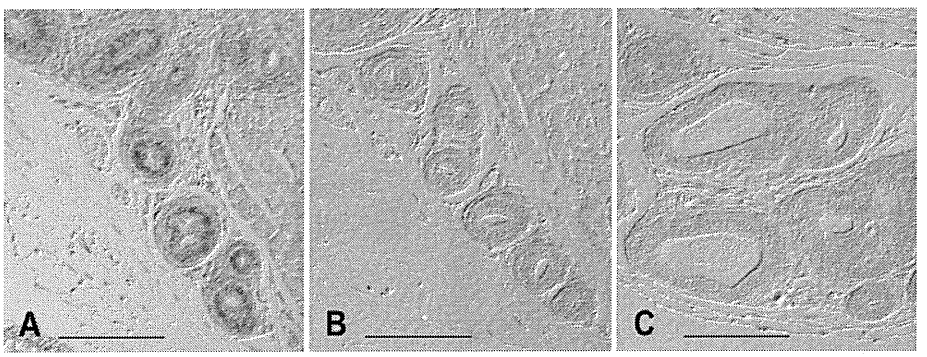

FIG. 3. In situ hybridization analysis of *Pbsn* mRNA expression in the dorsolateral prostate lobe of $Ahr^{+/+}$ mouse UGCs on PND14. **A**) Antisense probe for control mouse. **B**) Sense probe for control mouse. **C**) Antisense probe for TCDD-exposed mouse. Note that epithelial cells of the dorsolateral prostate lobes show *Pbsn* mRNA signals in control mice (**A**), but not in TCDD-exposed mice (**C**). Bar = 200 μm.

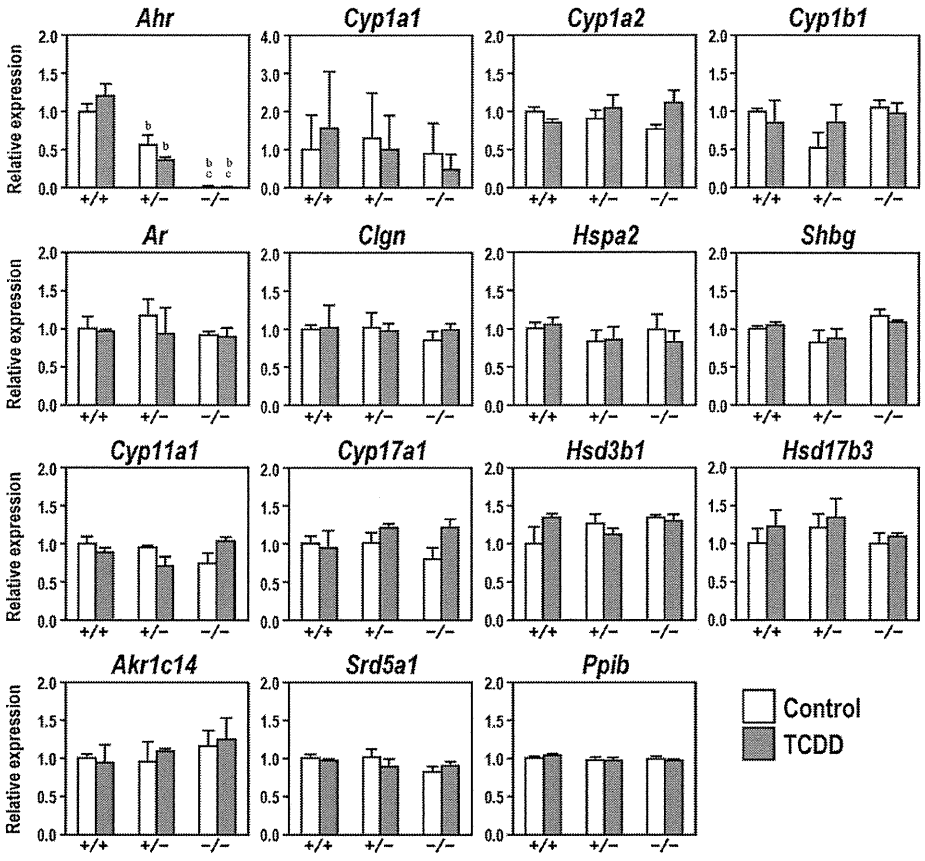

FIG. 4. Quantitative RT-PCR analysis of gene expression in the testes of male pups of three *Ahr* genotypes ($Ahr^{+/+}$, $Ahr^{+/-}$, and $Ahr^{-/-}$) on PND14 with or without TCDD exposure in utero. The values are expressed as the mean ± SE for three samples from each group. Significant differences were analyzed with ANOVA followed by the Fisher PLSD test (b, versus the same treatment of wild-type; c, versus the same treatment of heterozygous; $P < 0.01$).

Histopathology of the Testis

Spermatocytes at the pachytene stage proliferate from the spermatogonium on PND14, and calnexin-t is expressed at this stage [33]. In the present study, germ cells from the three mouse genotypes were immunostained for calnexin-t (Fig. 5, A–C). Positive cell populations were similar in control and TCDD-exposed testes from all genotypes (Fig. 5, D–F).

DISCUSSION

Ahr-*Dependent Reduction in Anogenital Distance and Impairment of Prostatic Development by In Utero and Lactational TCDD Exposure*

In this study, we demonstrated that in utero and lactational TCDD exposure caused reduction of the anogenital distance and impairment of prostatic development in an *Ahr*-dependent manner, because reduction of anogenital distance and disappearance of prostatic epithelial protein mRNAs were observed in $Ahr^{+/+}$ and $Ahr^{+/-}$ but not in the $Ahr^{-/-}$ offspring. The induction of *Cyp1a1* and *Cyp1b1* mRNAs was also observed in $Ahr^{+/+}$ and $Ahr^{+/-}$ mice but not in $Ahr^{-/-}$ mice. Taken together, impairment to the male reproductive system by in utero and lactational TCDD exposure was mainly dependent on the fetal *Ahr* gene.

A study using *Ahr* knockout mice that produced results similar to ours has been reported [17]. In that study, $Ahr^{+/-}$ female and $Ahr^{+/-}$ male mice were mated, and TCDD (5 μg/kg) was injected into the pregnant mice on GD13. The levels of prostatic protein markers were reduced in the TCDD-exposed $Ahr^{+/+}$ mice on PND90, but not in the $Ahr^{-/-}$ mice. Furthermore, those authors reported that TCDD administration on GD13 severely inhibited prostatic bud formation from the urogenital sinus in the fetus [28]. The use of in an vitro organ culture system as well as *Ahr* knockout mice revealed that the inhibition was mediated by AHR expressed in the mesenchy-

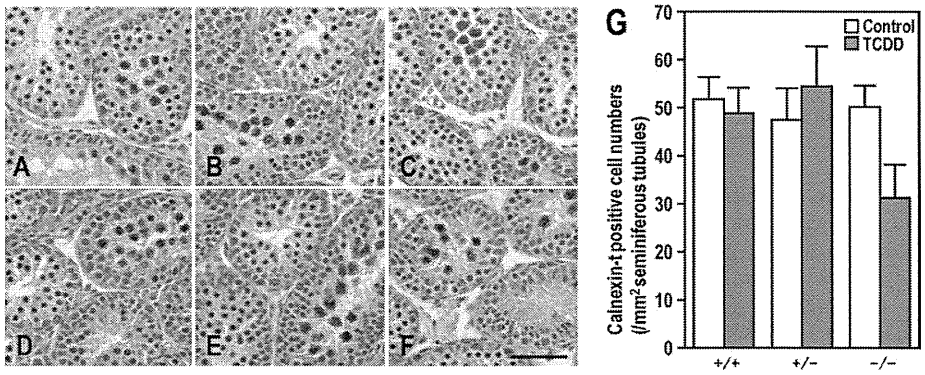

FIG. 5. Immunostaining of CLGN in the testes of male pups on PND14. Testis tissue preparations from each genotype (n = 3) were immunostained. **A**) Control $Ahr^{+/+}$ testis. **B**) Control $Ahr^{+/-}$ testis. **C**) Control $Ahr^{-/-}$ testis. **D**) TCDD-exposed $Ahr^{+/+}$ testis. **E**) TCDD-exposed $Ahr^{+/-}$ testis. **F**) TCDD-exposed $Ahr^{-/-}$ testis. CLGN-positive spermatocytes were observed in all genotypes and TCDD-treatment groups. **G**) Morphometric analysis. There were no statistical differences in the number of positive cells per testis cross section, for all genotypes and treatments. Bar = 100 μm.